ADDIS ABABA UNIVERSITY

SCHOOL OF GRADUATE STUDIES

FACULTY OF TECHNOLOGY

ELECTRICAL AND COMPUTER ENGINEERING

DEPARTMENT

DIGITAL IQ IMBALANCE COMPENSATION TECHNIQUES FOR OFDM RECEIVERS

By

Amare Assefa

A thesis submitted to the School of Graduate Studies of Addis Ababa University in partial fulfillment of the requirements for the degree of

Masters of Science

In

Electrical Engineering

Date: June 2007 G.C.

Addis Ababa, Ethiopia

ADDIS ABABA UNIVERSITY

SCHOOL OF GRADUATE STUDIES

FACULTY OF TECHNOLOGY

ELECTRICAL AND COMPUTER ENGINEERING

DEPARTMENT

DIGITAL IQ IMBALANCE COMPENSATION TECHNIQUES FOR OFDM RECEIVERS

By

Amare Assefa

Advisor

Dr.–Ing. Hailu Ayele

ADDIS ABABA UNIVERSITY

SCHOOL OF GRADUATE STUDIES

FACULTY OF TECHNOLOGY

ELECTRICAL AND COMPUTER ENGINEERING

DEPARTMENT

DIGITAL IQ IMBALANCE COMPENSATION TECHNIQUES FOR OFDM RECEIVERS

BY

Amare Assefa

APPROVAL BY BOARD OF EXAMINERS

Chairman Department of Graduate Committee	Signature
Advisor	Signature
Examiner	Signature
External Examiner	Signature

Declaration

I, the undersigned, declare that this thesis is my original work, has not been presented for a degree in this or any other university, and all sources of materials used for the thesis have been acknowledged.

Name: Amare Assefa

Signature: _____

Place: Addis Ababa

Date of submission: _____

This thesis has been submitted for examination with my approval as a university advisor.

Dr.-Ing. Hailu Ayele _____

Advisor's Name Signature

ACKNOWLEDGMENTS

I would like to express my sincere appreciation and deepest gratitude to my advisor Dr.Ing. Hailu Ayele for his constant support and invaluable guidance. I really appreciate his enthusiasm and integral view of the thesis and his quest for high-quality work.

My heartful appreciation also goes to Dr. Eneyew Adugna, Prof. Woldeghiorgis W. and Prof. D. Roy for their comments during the formulation of the thesis.

I would like to thank my family for their moral support and motivation during my studies. Words cannot describe my deep feeling of gratitude for my friend kalkidan Kassaye whose kindness and guidance have helped me pursue my goals in life. Special thank also goes to my sister Birtukan Assefa for her Moral support during my studies.

I would also like to thank all my friends for the great time we had together. In particular, I would like to thank all my friends in the Electrical and computer Engineering Department at AAU.

Finally, I would like to thank Ethiopian Telecommunication Corporation and Addis Ababa University for their material and financial support during my studies

TABLE OF CONTENTS

LIST OF FIGURES

LIST OF ACRONYMS

ADC	Analog to Digital Converter
AFC	Adaptive Frequency Correction
AWGN	Additive White Gaussian Noise
BER	Bit Error Rate
CFO	Carrier Frequency Offset
CP	Cyclic Prefix
DFT	Discrete Fourier Transform
DVB-T	European Digital Video Broadcasting system
FFT	Fast Fourier Transform
IEEE	Institute of Electrical and Electronics Engineers
IQ	Inphase and Quadrature phase
IF	Intermediate Frequency
IFFT	Inverse Fast Fourier Transform
ICI	Intercarrier Interference
ISI	Intersymbol interference
LO	Local Oscillator
LMS	Least Mean Square
LS	Least Squares
ML	Maximum Likelihood
MBWA	Mobile Broadband Wireless Access
ML	Maximum Likelihoods
OFDM	Orthogonal Frequency Division Multiplexing
PAPR	Peak-to-average Power Ratio
QAM	Quadrature Amplitude Modulation
QPSK	Quadrature Phase Shift Key
RF	Radio Frequency
SNR	Signal to Noise Ratio
VCO	Voltage Controlled Oscillator
VLSI	Very Large Scale Integration
WLAN	Wireless Local Area Network
WPAN	Wireless Personal Area Network
WMAN	Wireless Metropolitan Area Networks
ZIF	Zero Intermediate Frequency

ABSTRACT

With increasing demands for higher data rate and better services, more efficient modulation techniques such as orthogonal frequency division multiplexing (OFDM) are being adopted by many broadband wireless standards. However, the implementation of OFDM-based systems suffers from impairments such as in-phase and quadrature-phase (IQ) imbalances in the receiver front-end analog processing. IQ imbalance has been identified as a key front-end effect for OFDM systems. Such imbalances are caused by the analog processing of the radio frequency (RF) signal. The resulting IQ distortion limits the achievable operating SNR at the receiver and the achievable data rates. The IQ imbalances can severely limit the operating SNR and, consequently, the supported constellation sizes. This leads either to heavy front-end specifications and thus expensive front-end systems or large performance degradations.

The direct-conversion receiver is a potential solution offering a flexible architecture to cover multiple RF standards while simplifying the system design and reducing overall costs. However, IQ imbalance has been identified as one of the most serious concerns in the practical implementation of the direct conversion receiver architecture. A very promising approach for coping with these analog impairments is to compensate them digitally.

In this thesis, OFDM receiver with front-end analog impairments (such as IQ imbalance) is analyzed and descriptions of the physical sources of IQ imbalances are given. Based on the mathematical analysis an IQ imbalance model is developed. The development of model is based on the direct conversion receivers. Using the developed model, compensation algorithms in the digital domain is presented. Two alternative digital techniques are proposed and analyzed. The first one is based on Least Square (LS) method whereas the second method is based on Least Mean Square (LMS) method. Both compensation schemes use training to estimate the distortion parameters that model the IQ imbalances. The performance of both compensation methods is studied using computer simulation. The bit error rate (BER) versus SNR result indicates that the proposed methods can provide sufficient compensation performance with reasonable assumption.

CHAPTER ONE

INTRODUCTION

1.1 Background

Wireless communication has exhibited explosive growth in the past two decades and has become an essential part of everyday communication. It changed people's life style in every aspect. The growing acceptance and dependence on wireless communication has driven the need for higher data rates and stricter reliability requirements. To support the emerging information technology application, such as wireless sensors network, mobile computing, high speed mobile internet, and real time wireless multimedia application, high speed communications over broadband wireless channels has emerged as a key feature of future communications systems. The demand for higher information capacity in these and other similar applications has motivated the utilization of broadband wireless channels in order to provide higher data rates.

Orthogonal frequency division multiplexing (OFDM) is emerging as the modulation scheme for broadband communications. This is mainly motivated by the simple receiver structures for OFDM systems over broadband channels. Due to the recent advances of digital signal processing and Very Large Scale Integration (VLSI) technologies, the initial obstacles of OFDM implementation, such as massive complex multiplications and high speed memory accesses do not exist anymore. Mean while, the use of Fast Fourier Transform (FFT) algorithms eliminates arrays of sinusoidal generators and coherent demodulation required in parallel data systems and make the implementation of the technology cost effective.

OFDM based physical layers have already been chosen for several wireless systems such as the IEEE 802.11a wireless local area network (WLAN) in the 5GHz band [14], the recently adopted IEEE 802.11g wireless local area network (WLAN) in the 2.4GHz band [15], and the European digital video broadcasting system (DVB-T) [17]. It is also under consideration as the high rate alternate physical layer to the IEEE P802.15.3 wireless personal area network (WPAN) [18], the IEEE 802.20 mobile broadband wireless access (MBWA) [19] and the IEEE 802.16 wireless metropolitan area networks (WMAN) or WiMax [16].

Traditionally OFDM systems employ a Superheterodyne architecture to convert the baseband

signal to a Radio Frequency (RF) signal and vice-versa. The basis of this architecture is the step-wise up or down conversion, with dedicated filtering and amplification at each step, guaranteeing good selectivity and sensitivity. Thus, the Superheterodyne architecture delivers a signal with low distortion. It converts the RF signal down to digital baseband in several steps, passing via Intermediate Frequencies (IF). The drawback of this architecture, however, is that it requires a lot of components to reach this good signal quality. At each analog IF, the filters and the amplifier all add to the component cost. Not only are they quite expensive components, but as they are external, they also add to the assembling cost.

An alternative to the Superheterodyne architecture is the Zero-IF architecture (or Direct-Conversion architecture). As the name suggests, the Zero-IF architecture converts the RF signal directly to baseband or vice-versa without any IFs. This clearly results in a lower component count and consequently a lower cost. The Zero-IF architecture enables an easier integration and leads to a smaller form factor. Recently there has been a renewed interest in direct-conversion RF receivers that offer significant advantages in cost, package size, and power consumption [12].

OFDM based systems are very vulnerable to radio front-end induced impairments. One such impairment arises as a result of imbalances in the In-phase (I) and Quadrature-phase (Q) branches. This leads either to heavy front-end specifications and thus an expensive front-end or to large performance degradations. Although IQ imbalances are an issue to be addressed for both of these architectures, addressing the imbalances in the analog domain is more severe and challenging in the zero intermediate frequency (ZIF) or direct-conversion architecture [12].

The down-conversion to baseband in both architectures is implemented by what is known as complex down-conversion [12] see Figure 1.1. A complex down-converter basically multiplies the RF signal by the complex waveform $e^{-j2\pi f_{LO}t}$, where f_{LO} is the local oscillator frequency at the receiver.

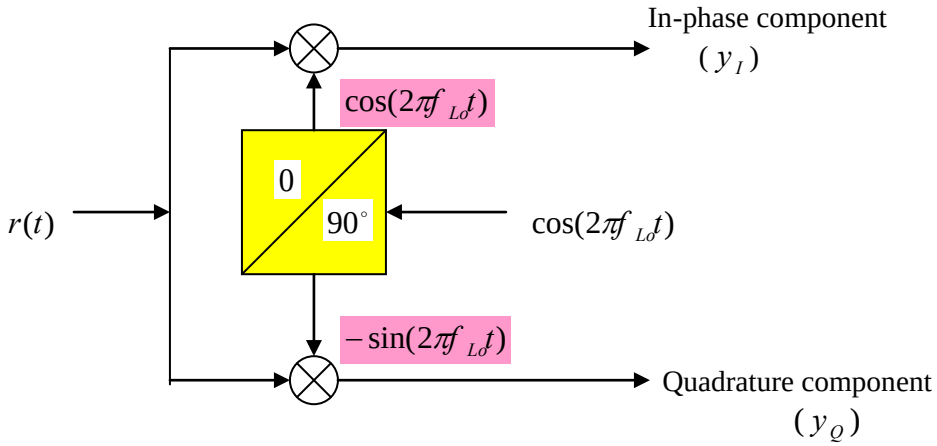

Figure 1.1, A complex down-conversion

To perform the complex down conversion both the sine and cosine waveforms are required (known as in-phase and quadrature-phase LO). As seen in Figure 1.1, in-phase LO, quadrature-phase LO and two mixers (multipliers) are required to perform the complex down-conversion. Furthermore, the receiver is divided to I and Q branches (representing the real and imaginary parts of the equivalent baseband signal). Each branch includes amplification, channel select filtering and digitization. The key fact to note is that the sine and cosine Waveforms at the receiver performing the down conversion need to be orthogonal, i.e., with exactly 90 degrees phase difference and with the same amplitude.

Achieving such orthogonal sinusoidal waveforms at radio frequencies as high as 5.2GHz (the band of operation for IEEE 802.11a) is a challenging task for silicon implementations [12]. Integrated circuit technologies, such as low-cost complementary metal-oxide semiconductor (CMOS) technology, have considerable mismatch between components due to fabrication process variations including doping concentration, oxide thickness, mobility and geometrical sizes over the chip [2][13]. Since analog circuits are sensitive to the component variations there will be unavoidable errors in the phases of LOs and gains of IQ branches due to process mismatches and temperature variations.

When the I and Q branches are perfectly matched, the image signal band is completely attenuated by the IQ processing [1]. In practical implementations, however, the matching of the I and Q branches can never be perfect [1][2]. As a consequence, the image band rejection provided by the IQ processing is finite and the desired channel signal is interfered by the image

signal. Any mismatch between the processing performed on the I and Q branches after down-conversion will contribute to an overall IQ imbalance in the system.

In general there are techniques developed in the analog domain to reduce such mismatches. Component mismatches are lowered by layout techniques and increasing the physical size of the devices to benefit from averaging over the area [3] [13]. Also different circuit topologies such as tunable polyphase, Voltage controlled oscillator (VCO), VCO with tunable polyphase have been used in analog circuit designs, which are more robust to component mismatches [12] [20]. However, such techniques suffer from different offsets, errors in the measurement feedback loop, and long time calibration process [7] [12]. Moreover, these techniques increase the device sizes and raise the power consumption in the analog domain. Even accepting the power consumption penalty does not remove the mismatches completely.

Any process variation in resistor or capacitor values causes them to introduce mismatches in the analog domain. Any layout parasitics and temperature variations can essentially limit the achievable match between the I and Q branches at high carrier frequencies [3] [12]. Indeed, with careful analog circuit design, phase imbalance of 1-2° and amplitude imbalance of 1-2% are realistic resulting in 30-40 dB attenuation of the image signal only[8][20]. This means that in the variety of low-cost and low-complexity implementations a non negligible degradation of the overall communication link performance arises if the above effect is not adequately compensated.

1.2 Motivation

The required specifications for systems such as IEEE 802.11a cannot be met purely based on analog domain techniques and without some type of digital compensation [5][6][7]. There are major advantages to compensating IQ imbalances in the digital domain. As is well-known, there is always a trade off in the analog domain between power, speed and area for precision [4] [12]. Such a trade-off does not exist in the digital domain with the same strength. The area and power consumption for digital processing scales down as the technology scales down, but the same trend does not hold for analog processing. Actually, the continuous interest in cost, power and size reduction of the portable communication systems has been encouraging the designers to integrate the analog front-end and the digital signal processing on the same chip die in CMOS technology[12].

Digital circuits are taking advantage of the technology scaling while the analog circuits are becoming more difficult to design efficiently in terms of power and area. As a result, there is an increasing interest in exploiting the digital processing power to alleviate the analog domain imperfections and in designing the analog and digital processing as a unified system, as opposed to the conventional separate analog-digital system design approach. This unification will allow designers to relax analog design requirements (and consequently the total cost and power) by moving more tasks into the digital domain.

In OFDM a cyclic prefix that is equal or longer than the channel delay spread is required to maintain orthogonality between subcarriers. This depends on the fact that ideal conditions are satisfied such as: no IQ imbalance, no carrier frequency offset and the channel is time-invariant over the OFDM block period. In practice, it is very difficult to satisfy all these conditions. This motivates us to search for alternative equalization techniques that are robust against these imperfections, mainly the IQ imbalances. In general, the motivation for the compensation approach presented in this thesis is as follows

1. As explained above, Perfect IQ match *is not* possible in the analog domain, especially when low cost fabrication technologies are used.

2. As higher data rates are targeted, higher constellation sizes and higher operating SNR are needed to support high density constellations. Higher SNR requirements translate to tougher IQ matching requirements.

3. As the carrier frequencies increase, the IQ imbalances become more severe and more challenging to eliminate [12]. The increase in carrier frequencies translates to higher IQ imbalances, and the trend in communications systems is to utilize more bandwidth and higher carrier frequencies.

4. The impairments in analog processing tend to increase as integrated circuit technologies, such as complementary metal-oxide semiconductor (CMOS) technology, are being more widely adopted for analog processing due to their cost advantage and ease of integration with digital baseband processing [4]

5. As will be shown in the next three chapters, the IQ distortion can be estimated and compensated in the *digital* domain.

For all the above reasons, it is desirable to develop reception techniques in the digital domain that help eliminate the effect of IQ imbalances in wireless receivers. Different digital approaches have been proposed to overcome the analog front-end problems for OFDM transmission. In [10] the author proposes a training based-technique for carrier frequency offset (CFO) estimation assuming perfect IQ balance. Maximum likelihood (ML) frequency offset estimation is proposed in [11], also assuming perfect IQ balance. On the other hand, as the carrier frequencies increase, the IQ imbalances become more severe and more challenging. Hence, techniques can be developed in the *digital domain* to track and eliminate IQ imbalances.

1.3 Objective

The general objective of this thesis is to study the effect of IQ imbalances on OFDM receivers and to investigate receiver algorithms for combating such distortions or imbalances through digital signal processing.

Specific objectives are:

- To analyze the OFDM systems with IQ imbalance and to develop IQ imbalance model.
- To propose least square (LS) and adaptive least mean square (LMS) receiver algorithms that compensate for IQ imbalance.
- To evaluate the proposed receiver algorithms in terms of bit error rate as a function of signal-to-noise ratio (SNR), simulation of a typical OFDM system with IQ imbalance *(no compensation)*, IQ imbalance with compensation *(proposed scheme*) and ideal IQ *(no IQ imbalance and prefect channel knowledge)* are made.

1.4 Outline of the Thesis

This thesis consists of six chapters. Chapter two describes the basic principles of OFDM system and its implementation impairment. In this chapter, a basic system model is given, common components for OFDM based systems are explained, and a simple transceiver based on OFDM modulation is presented. Important implementation impairments in OFDM systems are also discussed.

In Chapter three, the effect of IQ imbalance in OFDM system is analyzed. Based on the mathematical analysis, IQ imbalance model is developed. In this chapter, OFDM system with front end analog IQ imbalance is analyzed and discussed.

In chapter four, we develop compensation algorithms in the digital domain based on the analysis of chapter three. The algorithms include least square (LS) compensation, as well as an adaptive LMS compensation scheme with improved convergence rate.

Chapter five provide the results of the simulations of the proposed algorithm. In this chapter, discussion of the simulation result is also presented.

Finally, in chapter six, we draw the conclusions of the thesis and some suggestions for future works are presented.

CHAPTER TWO

OFDM SYSTEMS AND THEIR IMPLEMENTATION IMPAIRMENTS

In this chapter, after discussing a brief history of Orthogonal Frequency Division Multiplexing (OFDM), the basic principles of OFDM are introduced. A basic system model is given, common components for OFDM based systems are explained, and a simple transceiver based on OFDM modulation is presented. Important implementation impairments in OFDM systems are discussed.

2.1 History of OFDM

The history of OFDM dates back all the way to the mid 1960s, when Chang [21] published a paper on the synthesis of bandlimited orthogonal signals for multichannel data transmission. He presented a new principle of transmitting signals simultaneously over a bandlimited channel without ICI and ISI. Right after Chang's publication of his paper, Saltzburg [22] demonstrated the performance of an efficient parallel data transmission system in 1967, and he concluded that the strategy of designing an efficient parallel system should concentrate on reducing crosstalk between adjacent channels than on perfecting the individual channels themselves. His conclusion has been proven far-sighted today in the digital baseband signal processing to combat the ICI.

In the developments of OFDM technology, there are two remarkable contributions to the technology which transform the original analog multicarrier system to today's digitally implemented OFDM. The use of DFT (discrete Fourier transform) to perform baseband modulation and demodulation was the first milestone when Weinstein and Ebert [23] published their paper in 1971. Their method eliminated the banks of subcarrier oscillators and coherent demodulators required by frequency-division multiplexing and hence reduced the cost of OFDM systems. This presented an opportunity for an easy implementation of OFDM, especially with the use of Fast Fourier Transform (FFT), which is an efficient implementation of the DFT. This suggested that the easiest implementation of OFDM is with the use of Digital Signal Processing (DSP), which can implement FFT algorithms. In their paper [23], they used a guard interval between consecutive symbols and the raised-cosine windowing in the time domain to combat the ISI and the ICI. But their system could not keep perfect orthogonality between subcarriers over a time dispersive channel.

Another important contribution was due to Peled and Ruiz in 1980[35], who introduced the cyclic prefix (CP) or cyclic extension, solving the orthgonality problem. Instead of using an empty guard space, they filled the guard space with the cyclic extension of the OFDM symbol. This effectively simulates a channel performing cyclic convolution, which maintains orthgonality over dispersive channels when the CP is longer than the impulse response of the channel. Though this introduces an energy loss proportional to the length of CP when the CP part in the received signal is removed, the zero ICI generally pays for the loss. Recently, OFDM has been widely adopted and implemented in wire and wireless communication. Following the above brief historical overview of OFDM developments, issues related to implementations OFDM will be discussed in more detail.

2.2 Basic principles OFDM Systems

2.2.1 Introduction

OFDM is a multicarrier transmission technique, which divides the available spectrum into a number of sub channels, each one being modulated by a low rate data stream. In this sense, OFDM is similar to a classical parallel data transmission system with non-overlapping frequency sub channels. However, OFDM uses the spectrum more efficiently by spacing the channels much closer to each other, see Figure 2.1. This is achieved by making all the sub carriers orthogonal to each other. The orthogonality of the carriers means that each carrier has an integer number of cycles over a symbol period. Due to this, at the maximum of each carrier spectrum, all the other carriers' spectrum has a null, which results in no interference between the adjacent spaced channels.

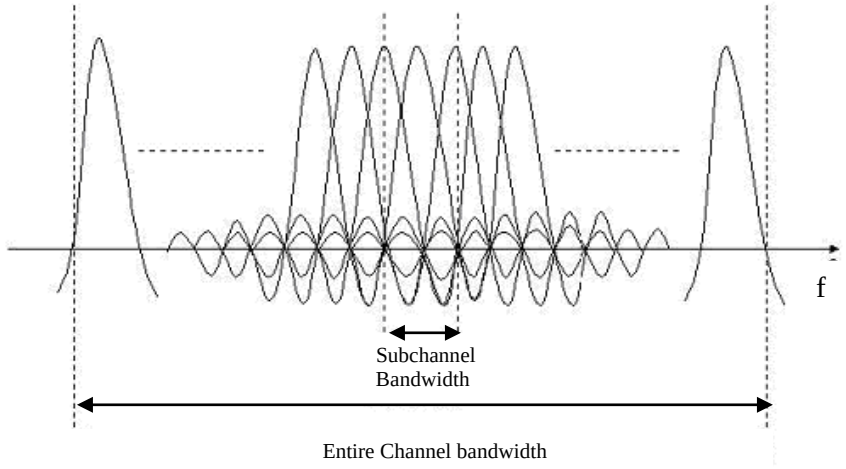

Figure 2.1, Spectra of individual subcarriers that are allocated orthogonally to each other.

One of the most attractive features of OFDM is its robustness against frequency selective channels. The OFDM operation converts a frequency selective channel into multiple parallel flat fading channels, which greatly simplifies the channel estimation and equalization tasks at the receiver. OFDM is bandwidth efficient since the subchannels can overlap yet still be separated due to the use of orthogonal subcarriers. With the current advancements in digital signal processor (DSP) and integrated circuit (IC) technology, OFDM can be efficiently implemented by using the inverse fast Fourier transform (IFFT) and fast Fourier transform (FFT) for modulation and demodulation respectively. Although OFDM exhibits a high spectral efficiency, it has several disadvantages when compared with traditional single carrier systems. These disadvantage lie mainly in the constraints it put on the quality of the analogue radio frequency (RF) front-end of both transmitter and receiver [24].

2.2.2 System Model

OFDM is a block transmission technique. In the baseband, complex-valued data symbols modulate a large number of tightly grouped carrier waveforms. The transmitted OFDM signal multiplexes several low-rate data streams. Each data stream is associated with a given subcarrier. The main advantage of this concept in a radio environment is that each of the data streams experiences an almost flat fading channel. In slowly fading channels, the intersymbol interference (ISI) and intercarrier interference (ICI) within an OFDM symbol can be avoided with a small loss of transmission energy using the concept of a cyclic prefix.

2.2.2.1 Transmitter

The discrete-time baseband equivalent model of the OFDM system under consideration is shown in Figure 2.2. The blocks on the top row correspond to components in the transmitter and those in the bottom row to the receiver. The input data stream is modulated using regular modulation techniques such as phase shift keying (PSK) or quadrature amplitude modulation (QAM). The modulated signal $X(k), (k = 0, 1, \ldots N$, where N is the number of subcarriers) is converted into parallel signals and passed to the IFFT block.

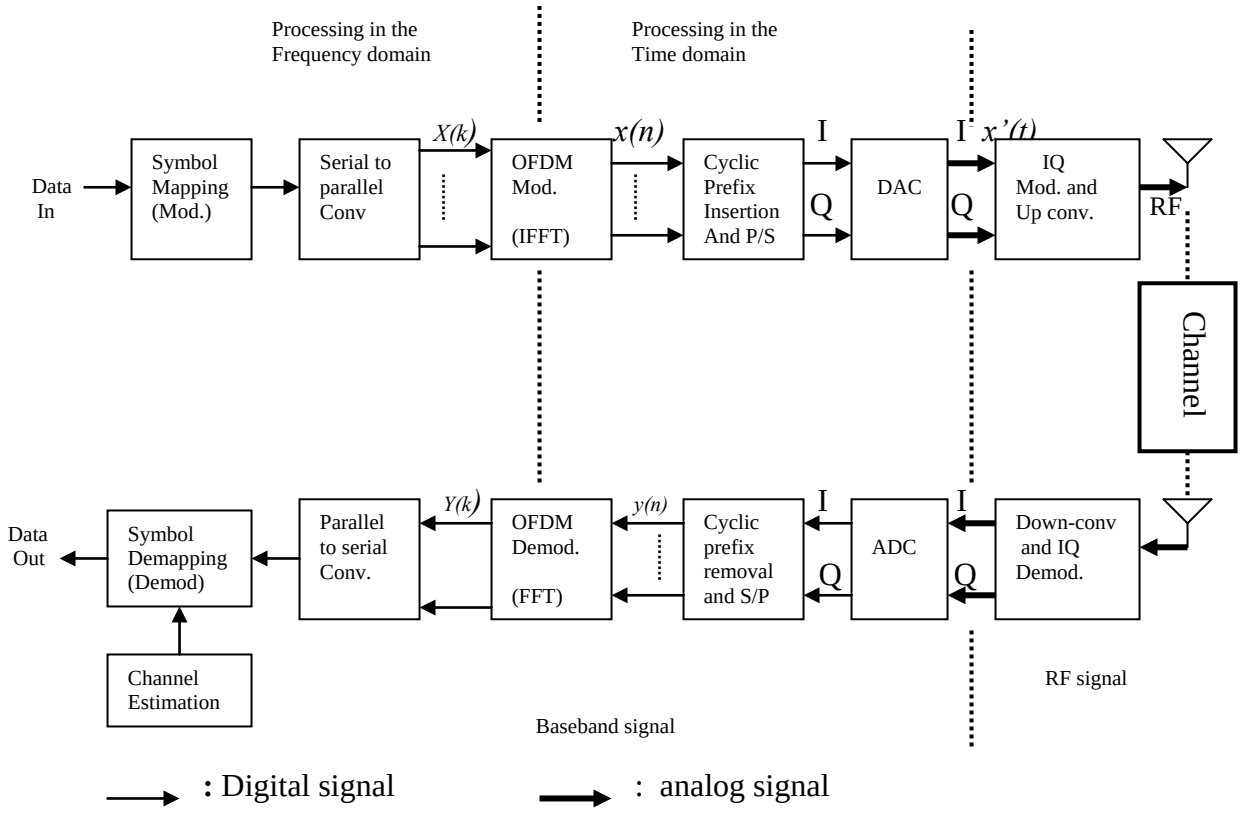

Figure 2.2, Baseband equivalent model of OFDM

The IFFT operation modulates the parallel signals onto orthogonal subcarriers as a group. The narrowband signal outputs are $x(n)$ where,

$$x(n) = IDFT\{X(k)\} = \frac{1}{\sqrt{N}} \sum_{k=0}^{N-1} X(k) e^{j2\pi nk/N}, \qquad 0 \le n \le N-1 \tag{2.1}$$

If, for example, a 64-point IFFT is used, the coefficients 1 to 26 are mapped to the same numbered IFFT inputs, while the coefficients –26 to –1 are copied into IFFT inputs 38 to 63. The rest of the inputs, 27 to 37 and the 0 (dc) input, are set to zero [14]. This mapping is illustrated in Figure 2.3. After performing an IFFT, the output is cyclically extended to the desired length.

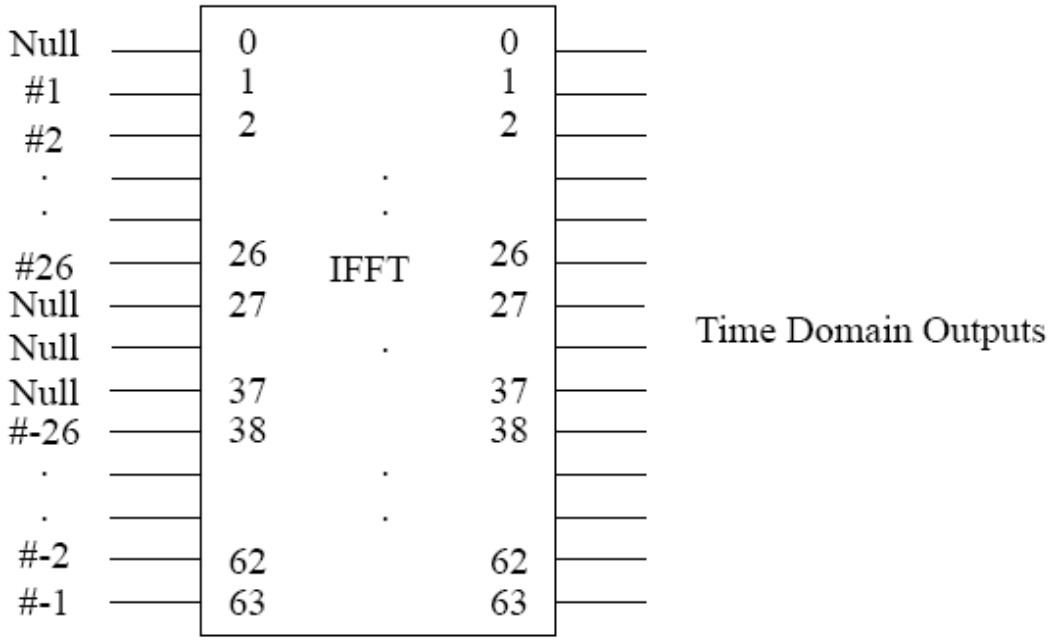

Figure 2.3, Inputs and outputs of IFFT

2.2.2.2 Cyclic extension of OFDM symbol

When transmitting several OFDM symbols in series there is a risk of interference between adjacent symbols caused by multipath propagation. To avoid this intersymbol interference (ISI), a guard interval is inserted between every OFDM symbol. During this guard interval the multipath components of the transmitted symbols should die out before the next OFDM symbol is transmitted. The guard time is chosen larger than expected channel delay spread, such that multipath components from one symbol cannot interfere with the next symbol.

To eliminate ICI, the OFDM symbol is cyclically extended in the guard time as shown in figure 2.4. The last part of the OFDM symbol is added in front of the transmitted symbol. This cyclic prefix (CP) converts the linear convolution of the transmitted symbol and the channel to a cyclic convolution and thus makes the DFT of the received signal to simply be the product of the complex symbol *x(n)* and the frequency response of the channel, provided that the length of the CP is greater than or equal to the channel delay spread.

This ensures that delayed replicas of the OFDM symbol always have an integer number of cycles within the FFT interval, as long as the channel delay is smaller than the guard time. As a result, multipath signals with delays smaller than guard time cannot cause ICI.

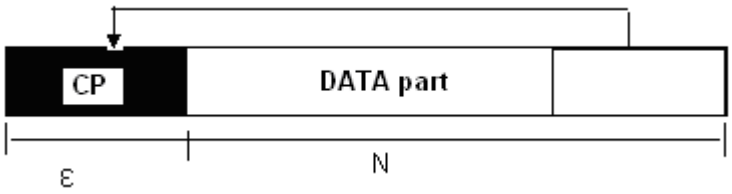

Figure 2.4, Shows the addition of the cyclic prefix where N is the length of the OFDM symbols and ε is the length of the cyclic prefix. The transmitted signal will then have the length N+ ε.

2.2.2.3 Channel model

Physical radio channels are characterized by multipath propagation. The transmitted signal is reflected, diffracted or scattered by objects surrounding the receiver. Thus the same signal arrives at the receiver through different paths with different amplitudes, different phases, and different time delays. One effect of this multipath propagation is that it causes the received signal to fade. This happens when delayed versions of the transmitted signal add destructively at the receiver due to their carrier frequency phase differences. For high speed communication systems, multipath propagation also causes intersymbol interference (ISI) because the differences between path delays are comparable to or larger than the symbol interval so that the time dispersion cannot be neglected.

For mobile communications, the transmitter, receiver, and the media are usually changing over time in unpredictable ways and therefore transmitted signals are attenuated and dispersed in time in a random manner. In order to achieve coherent demodulation, the channel conditions have to be measured and updated constantly during the process of reception.

In this thesis a multipath fading environment is considered and the block fading channel is assumed, i.e. the channel remains constant for one data packet length and changes to other independent value for the next packet length. Within one data packet, the channel is modeled by an FIR linear system as shown in figure 2.5.

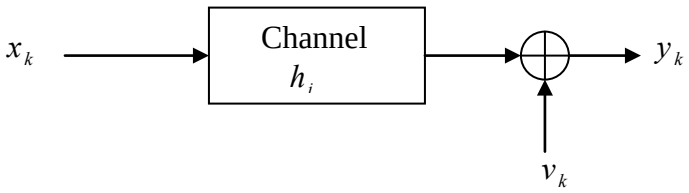

Figure 2.5, channel model

$$y_k = \sum_{i=0}^{\varepsilon} h_i x_{k-i} + v_k, \quad 0 \le k \le N-1 \qquad (2.2)$$

Where y_k is received signal, $\mathbf{h} = [h_0, h_1, ..., h_\varepsilon]^T$ is a channel vector, x_k is the input symbol and v_k is complex Gaussian noise with zero mean and variance σ^2. Note that the symbol ^{T} in channel vector denotes the transpose of the vector.

2.2.2.4 Receiver

After passing through inverse fast Fourier transform block and introduction of cyclic prefix, the OFDM modulated signal is converted to analog signal, $x'(t)$ using digital to analog converter (DAC) as shown in the figure 2.2. Then, it is upconverted by multiplication with local oscillator (LO) signal at the mixer. Next, The transmitted signal is filtered by the channel impulse response $h(t)$ and corrupted by additive noise. Consequently, the received signal, $y(t)$ is written as:

$$y(t) = x'(t) * h(t) + v(t) \qquad (2.3)$$

Where *v(t)* is the additive white Gaussian noise (AWGN).This signal is down-converted to remove the high frequency components and filtered.

The A/D converter samples the resulting signal to obtain

$$y[n] = x'[n] * h[n] + v[n], \quad -\varepsilon \le n \le N-1. \qquad (2.4)$$

The prefix of $y[n]$ consisting of the first ε samples is then removed. These time samples are serial-to-parallel converted and passed through an FFT. The FFT does just the inverse of the IFFT. The FFT is used to demodulate the N subcarriers of each of the received OFDM symbols.

It converts the time domain symbols at its input into frequency domain symbols at its output.

The N-point DFT (Discrete Fourier Transform) is defined as

$$Y(k) = DFT(y(n)) = \frac{1}{\sqrt{N}} \sum_{n=0}^{N-1} y(n) e^{-j(2\pi/N)kn}, \quad 0 \le k \le N-1 \tag{2.5}$$

The output of the DFT contains N QAM symbols (if QAM was used to modulate the data). However, the values of these N subcarriers contain random phase shifts and amplitude variations caused by analog front end imperfection and frequency selective fading. As a result of these phase shifts and amplitude changes, received symbols can be incorrectly demodulated. In order to be able to coherently detect the QAM symbols with estimate of bits as much as possible, knowledge about the reference phase and amplitude of each subcarrier is required. This task is carried out by the estimation and compensation of channel and analog front end imperfection, which is the motivation of this thesis.

2.3 Implementation impairments

OFDM based systems are very vulnerable to radio front-end induced impairments. Since stringent specifications for the front-end of the OFDM are required, the analogue part is the most expensive part of the system [24]. In this section, we first review issues related to IQ imbalance which is a core of this thesis. Following that, carrier frequency synchronization is introduced. Finally, we discuss high peak-to-average power ratios inherent to OFDM which puts tight requirements on the power amplifier design. Many aspects regarding frequency synchronization and the peak power problem are only described briefly here, since they are beyond the scope of this thesis.

2.3.1 IQ imbalance

Down-conversion is a fundamental stage in all radio frequency (RF) front-end architectures. In this process, the high carrier frequency (f_c) signal is multiplied by the outputs of the local oscillating signals (LO) and transferred to intermediate frequencies (f_{IF}) appropriate for further

amplification and processing, and eventually to the baseband. There are different architectures to convert an RF signal to baseband, either through an intermediate frequency (IF) or by direct down-conversion to baseband signal (zero intermediate frequency).

Traditionally OFDM systems employ a Superheterodyne architecture to convert the baseband signal to a Radio Frequency (RF) signal and vice-versa. The basis of this architecture is the step-wise up or down conversion, with dedicated filtering and amplification at each step, guaranteeing good selectivity and sensitivity. Thus, the Superheterodyne architecture delivers a signal with low distortion.

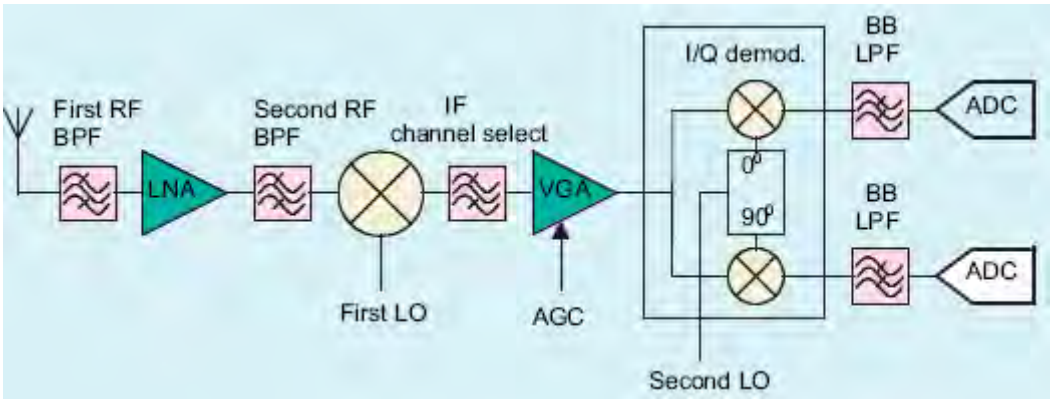

Figure 2.6, The simplified block diagram of superheterodyne receiver shows that the received RF signal goes through the first preselection filter to remove out-of-band signals and is then amplified by the low-noise amplifier.

It converts the RF signal down to digital baseband in several steps, passing via Intermediate Frequencies (IF).The drawback of this architecture, however, is that it require filters at the radio frequency (RF) and the intermediate frequency (IF) which can usually only be implemented by bulky surface acoustic wave (SAW) or crystal filters. Which means it requires a lot of components to achieve good signal quality. At each analog IF, the filters and the amplifier all add to the component cost. Not only are they quite expensive components, but as they are external, they also add to the assembling costs [2].

An alternative to the Superheterodyne architecture is the Zero-IF architecture (or Direct-Conversion architecture) shown in figure 2.7.

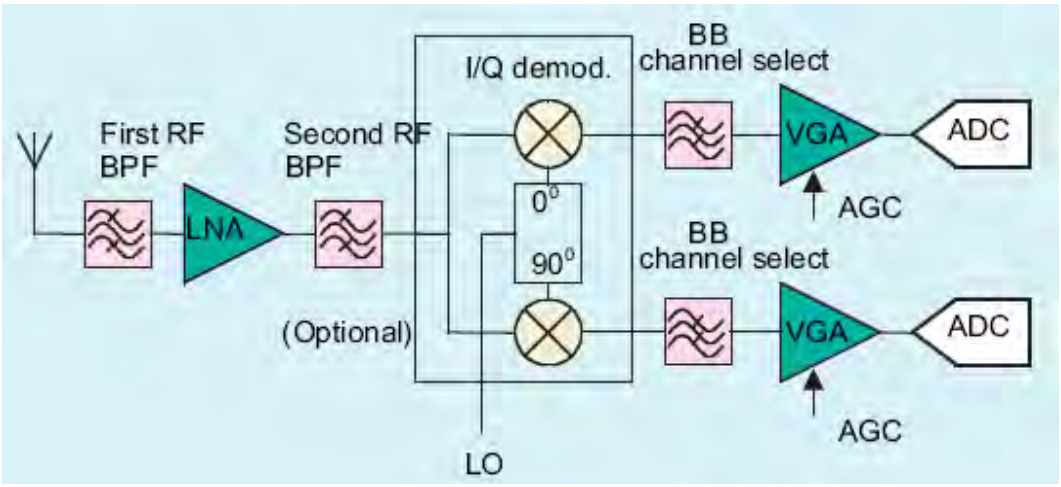

Figure 2.7, Direct-conversion receiver, the received signal is amplified with a fixed-gain LNA after the first RF preselection filter.

As the name suggests, the Zero-IF architecture converts the RF signal directly to baseband or vice-versa without any IFs. This clearly results in a lower component count and consequently a lower cost. The Zero-IF architecture enables an easier integration and leads to a smaller form factor. As a result, more of the future RF designs tend to be adopting this scheme.

However there are also drawbacks in using a Zero-IF architecture. Direct-conversion receivers need a local oscillator with in-phase and quadrature outputs for demodulation. It performs IQ demodulation in the analog domain. As a result the matching between the analog I and Q paths and their components are imperfect. The greater challenge in direct-conversion is to produce accurate quadrature phases with good amplitude match at the much higher *carrier-frequency* [12]. This leads to IQ imbalance distortion which significantly degrades the signal quality as it will be shown in subsequent chapters. Furthermore, with large signal constellations of *M*-QAM or M-PSK even modest *IQ* imbalances results in detrimental performance degradation.

The effect of receiver IQ imbalances on OFDM systems and the resulting performance degradation have been investigated in [26] [27]. To review some basic concepts, let us consider the OFDM block diagram shown on figure 2.2. Digital data is transferred in an OFDM link by using a modulation scheme on each subcarrier. A modulation scheme is a mapping of data words to a real (In phase) and imaginary (Quadrature) constellation, also known as an IQ constellation. For example 16-QAM (Quadrature Amplitude Modulation) has 16 IQ points in the constellation, constructed in a square with 4 evenly spaced columns along the real axis and 4 rows along the

imaginary axis. The number of bits that can be transferred using a single symbol corresponds to log2 (M), where M is the number of points in the constellation, thus 16-QAM transfers 4 bits per symbol.

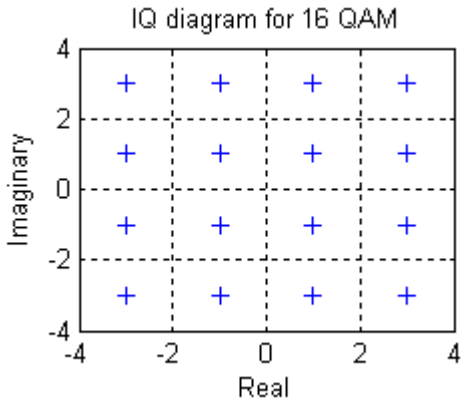

Figure 2.8, IQ modulation constellation for 16-QAM with gray coding of the data to each location.

Each data word is mapped to one unique IQ location in the constellation. The resulting complex vector $I + jQ$ corresponds to an amplitude of $\sqrt{I^2 + Q^2}$ and a phase of $\angle(I + jQ)$ Where $j = \sqrt{-1}$. In the receiver, mapping the received IQ vector back to the data word performs subcarrier demodulation. During transmission, noise and distortion becomes added to the signal due to thermal noise, signal power reduction, analog components mismatch and imperfect channel equalizations. In order to illustrate this, a typical OFDM system shown in figure 2.2 is simulated in the presence of AWGN and very small IQ mismatch. Figure 2.9 below shows an example of a received 16-QAM signal with a SNR of 25 dB.

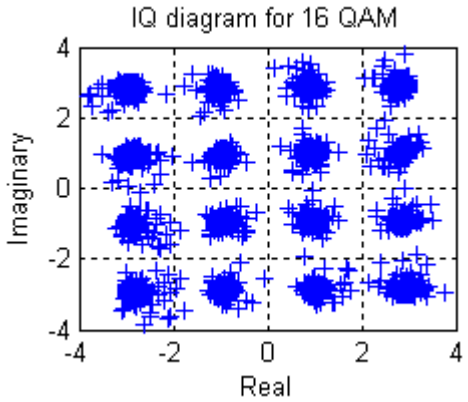

Figure 2.9, IQ plot for 16-QAM received data with added noise.

Similar result is also shown in [8].Each of the IQ points is blurred in location due to the channel noise and analog components imperfection. For each received IQ vector the receiver has to estimate the most likely original transmitted vector. This is achieved by finding the transmitted vector that is closest to the received vector. Errors occur when the noise exceeds half the spacing between the transmitted IQ points, making it cross over the decision boundary.

Increasing the number of points in the constellation does not change the bandwidth of the transmission, thus using a modulation scheme with a large number of constellation points, allows for improved spectral efficiency. For example 16-QAM has a spectral efficiency of 4 b/ s /Hz, as compared with only 1b/ s /Hz for BPSK. However, the greater the number of points in the constellation, the harder they are to resolve at the receiver. As the IQ locations become spaced closer together, it only requires a small amount of noise to cause errors in the transmission, which implies IQ imbalance is a critical problem in the implementation of high data rate OFDM systems

Both analog and digital methods for dealing with *IQ* imbalances have been reported in the literature. Different circuit topologies and architectures have been used in analog circuit designs, which are more robust to component mismatches.

In 1997 Rudell [31] used an individual tuning approach with a monolithic receiver.

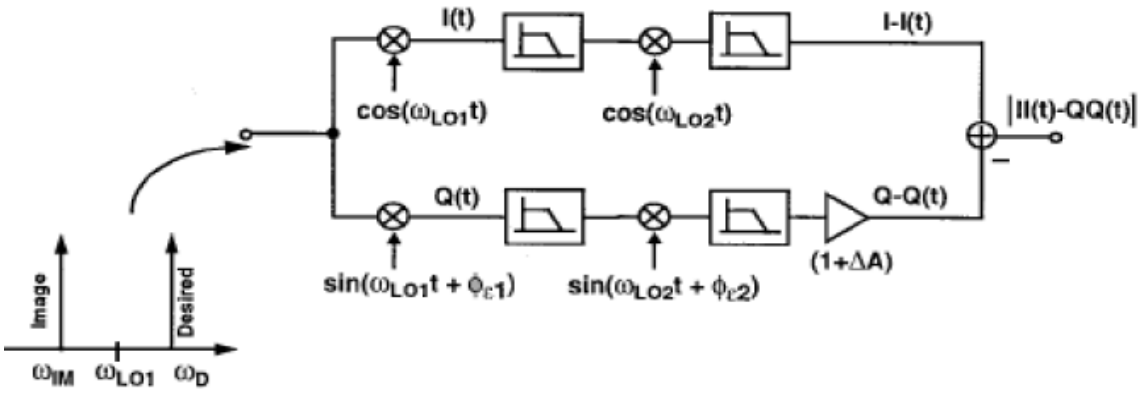

Figure 2.10, Image-Reject Mixer using Weaver architecture [31].

The gain mismatch between the I and Q channels could be tuned with a variable gain amplifier and the phase mismatch could be adjusted by varying the phase of the second local oscillator.

In 1999 Long and Maliepaard used layout techniques [29]. Their dual doubly-balanced mixer architecture used common-centroid and symmetric layout techniques to improve the matching enough to replace the external interstage image-reject filter used in typical heterodyne receivers.

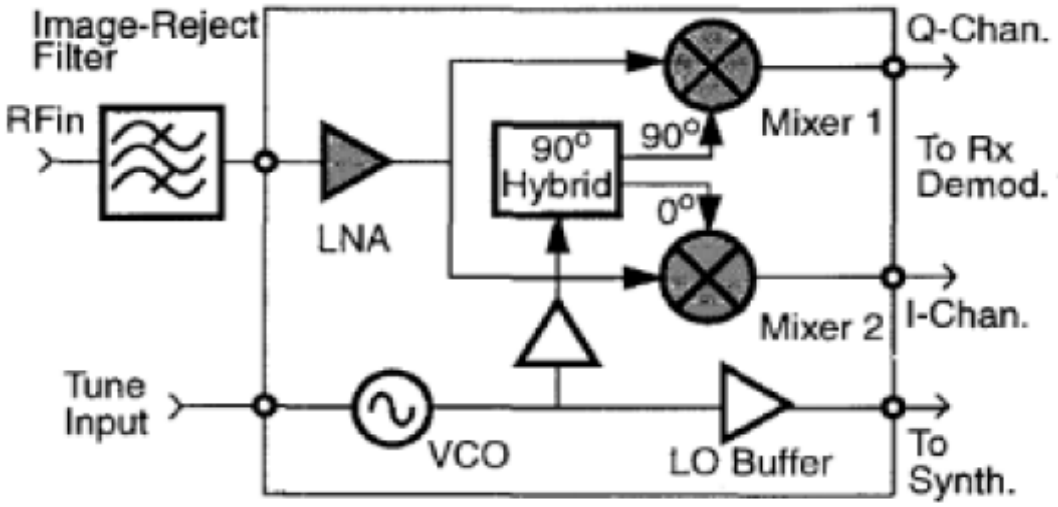

Figure 2.11, Dual doubly-balanced mixer architecture used for image rejection with good lay out matching [29].

While good layout is required, the degree of matching achieved is not enough to meet the image-rejection requirements of most standards without additional external filtering or additional calibration

In [28] trimming is used to adjust the amplitude and phase between the I and Q signals at IF to calibrate for the mismatch. The phase angle between the LO signals was then adjusted by setting a bias current ratio to produce a phase tuning relatively independent of frequency. The amplitude errors at the output of the receiver were compensated by varying the gain.

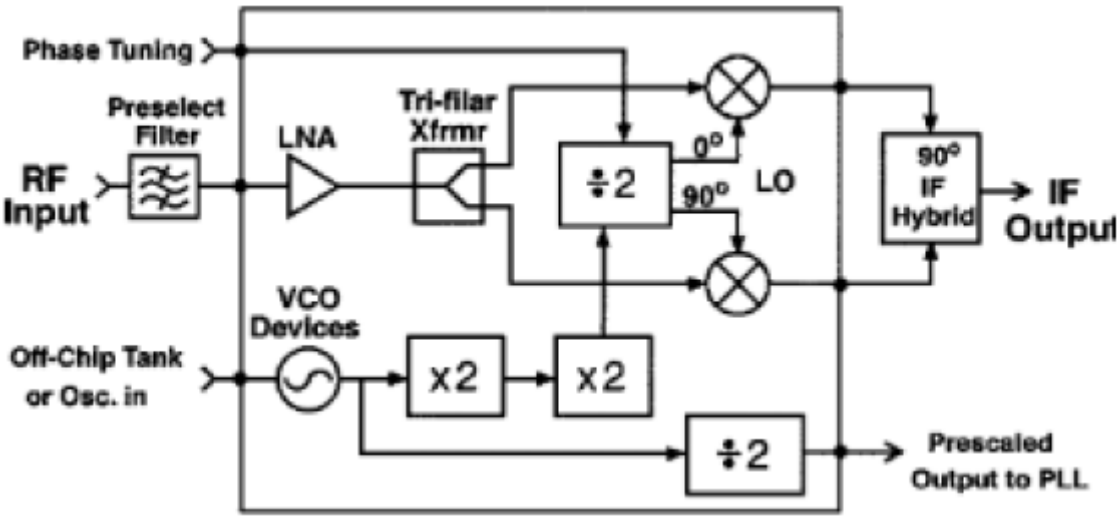

Figure 2.12, Image-Reject Receiver front end block diagram [28]

Hand tuning or trimming greatly increases the production costs [7]. For a commercial receiver an automatic method to perform the tuning on-chip is needed. Another analog calibration technique for an image-rejection receiver was introduced in 2000 by Montemayor and Razavi [30]. This calibration detects phase and gain mismatches and drives them to zero with a negative-feedback loop. It has very limited applications due to the high cost, long calibration time, and one-time nature of the calibration [7] [30]. It has also limited accuracy and excessive power consumption. In direct conversion receiver, the imbalance in IQ amplitude is corrected by adjusting the drain currents through the mixer transducer elements [5]. However this method has only a moderate effect on the channel phase balance.

In general, the occurrence of IQ imbalance can be circumvented by increasing the accuracy of the implemented mixing structure, which would result into a more expensive solution. In addition, these analog techniques increase the device sizes and raise the power consumption in the analog domain.

Rather than decreasing IQ imbalance by increasing the design time and the component cost, IQ imbalance can be compensated digitally. The challenge of a digital compensation is an accurate estimation of the parameters of the IQ imbalance. Different concepts for the digital estimation and compensation of the IQ imbalance in OFDM direct conversion receivers have been proposed

in [8] [25]. The simplest one is to estimate the imbalance parameters by feeding the receiver off-line with a calibration signal [25]. More advanced approaches use common blind signal separation algorithms, such as interference cancellation (IC) [8], [25] and blind source separation (BSS) [8]. Although leading to significant improvement under specific receiving conditions, these methods come with particular inherent drawbacks which are mainly the signal leakage problem and high cost [8] [25].

In this thesis, we propose training based digital baseband signal processing techniques to compensate for IQ imbalance

2.3.2 Frequency Offset

Frequency offset is one of the critical factors in OFDM system design. It results in inter-carrier interference (ICI) and degrades the orthogonality of sub-carriers. Frequency errors will tend to occur from two main sources. These are local oscillator errors and common Doppler spread. Any difference between transmitter and receiver local oscillators will result in a frequency offset.

Let us consider figure 2.2. Assume that we have the symbols *X(k)* to be transmitted using an OFDM system. These symbols are transformed to the time domain using IDFT as shown earlier in (2.1). This baseband signal (OFDM symbol) is then up-converted to RF frequencies and transmitted over the wireless channel. In the receiver, the received signal is down-converted to baseband. But, due to the frequency mismatch between the transmitter and receiver, the received signal has a frequency offset. This signal is denoted as *y(n).* The frequency offset is added to the OFDM symbol in the receiver. Finally, to recover the data symbols, DFT is applied to the OFDM symbol taking the signal back to frequency domain. Let *Y (k)* denote the recovered data symbols.

This process is shown below.

$$X(k) \xrightarrow{IDFT} x(n) \xrightarrow{frequencyoffset} y(n) \xrightarrow{DFT} Y(k) \qquad (2.6)$$

The effect of frequency offset on *x(n)* will be a phase shift of $\frac{2\pi\Delta fn}{N}$ where Δf is the normalized frequency offset.

Therefore,

$$
\begin{aligned}
y(n) &= x(n) \times e^{j\frac{2\pi\Delta f n}{N}} \\
&= \frac{1}{\sqrt{N}} \sum_{k=0}^{N-1} X(k) e^{j\frac{2\pi k n}{N}} \times e^{j\frac{2\pi\Delta f n}{N}} \\
&= \frac{1}{\sqrt{N}} \sum_{k=0}^{N-1} X(k) e^{j\frac{2\pi n}{N}(k+\Delta f)} \qquad (2.7)
\end{aligned}
$$

Finally, we need to apply DFT to *y(n)* with a view toward recovering the symbols.

$$
\begin{aligned}
Y(k) &= DFT(y(n)) \\
&= \frac{1}{N} \sum_{n=0}^{N-1} \Big\{ \sum_{m=0}^{N-1} X(m) e^{j\frac{2\pi n}{N}(m+\Delta f)} \Big\} e^{-j\frac{2\pi k n}{N}} \\
&= \frac{1}{N} \sum_{n=0}^{N-1} \sum_{m=0}^{N-1} X(m) e^{j\frac{2\pi n}{N}(m-k+\Delta f)} \qquad (2.8) \\
&= \frac{1}{N} \sum_{m=0}^{N-1} X(m) \Big\{ \sum_{n=0}^{N-1} e^{j\frac{2\pi n}{N}(m-k+\Delta f)} \Big\} \qquad (2.9)
\end{aligned}
$$

The term within the curly braces can be calculated using geometric series expansion,

$s_n = \sum_{k=0}^{n} r^k = \frac{1-r^{n+1}}{1-r}$. Using this expansion, we have

$$
\begin{aligned}
Y(k) &= \frac{1}{N} \sum_{m=0}^{N-1} X(m) \frac{1 - e^{j2\pi(m-k+\Delta f)}}{1 - e^{j\frac{2\pi(m-k+\Delta f)}{N}}} \qquad (2.10) \\
&= \frac{1}{N} \sum_{m=0}^{N-1} X(m) \frac{e^{j\pi(m-k+\Delta f)} (e^{-j\pi(m-k+\Delta f)} - e^{j\pi(m-k+\Delta f)})}{e^{j\frac{\pi(m-k+\Delta f)}{N}} (e^{-j\pi(\frac{m-k+\Delta f}{N})} - e^{j\pi\frac{\pi(m-k+\Delta f)}{N}})} \qquad (2.11) \\
&= \frac{1}{N} \sum_{m=0}^{N-1} X(m) \frac{e^{j\pi(m-k+\Delta f)} - 2j\sin(\pi(m-k+\Delta f))}{e^{j\frac{\pi(m-k+\Delta f)}{N}} - 2j\sin(\frac{\pi(m-k+\Delta f)}{N})} \qquad (2.12)
\end{aligned}
$$

$$\approx \sum_{m=0}^{N-1} X(m) e^{j\pi(\frac{(m-k+\Delta f)(N-1)}{N})} \frac{\sin(\pi(m-k+\Delta f))}{\pi(m-k+\Delta f)} \quad (2.13)$$

$$\approx \sum_{m=0}^{N-1} X(m) \frac{\sin(\pi(m-k+\Delta f)}{\pi(m-k+\Delta f)} e^{j\pi(m-k+\Delta f)} \quad (2.14)$$

In the above derivation we used the fact that sin(x) = x for small x values, and $\frac{N-1}{N} \approx 1$ for large N. If we define,

$$S(m,k) = \frac{\sin(\pi(m-k+\Delta f)}{\pi(m-k+\Delta f)} e^{j\pi(m-k+\Delta f)} \quad (2.15)$$

$$Y(k) = \sum_{m=0}^{N-1} X(m) S(m,k) \quad (2.16)$$

$$= X(k)S(k,k) + \sum_{m=0, m\neq k}^{N-1} X(m)S(m,k) \quad (2.17)$$

The first term in (2.17) is equal to the originally transmitted symbol shifted by a term that corresponds to Δf. This term, *S(k,k),* introduces a phase shift of $\pi\Delta f$ and an attenuation of $\frac{\sin(\pi\Delta f)}{\pi\Delta f}$ in magnitude. Actually, this term only depends on the value of offset Δf, but not carrier index k, so the effect of frequency offset on each sub carrier will be the same. The second term in (2.17) represents the interference from other sub-carriers.

This offset is usually compensated for by using adaptive frequency correction (AFC). However any residual (uncompensated) errors result in a degraded system performance. The amount of degradation is proportional to the fractional frequency offset which is equal to the ratio of frequency offset to the carrier spacing. Frequency offset can be estimated by different methods e.g. using pilot symbols, the statistical redundancy in the received signal, or transmitted training sequences [10][11][34].

2.3.3 Peak-to-Average Power Ratio

One of the major drawbacks of OFDM is its high Peak-to-average Power Ratio (PAPR). Superposition of a large number of subcarrier signals results in a power density with Rayleigh distribution which has large fluctuations [33]. OFDM transmitters therefore require power amplifiers with large linear range of operation which are expensive and inefficient. Any amplifier non-linearity causes signal distortion and inter-modulation products resulting in unwanted out-of-band power and higher BER [32]. The Analog to Digital converters and Digital to Analog converters are also required to have a wide dynamic range which increases complexity [33].

A large PAPR brings disadvantages like an increased complexity of the analog-to-digital converters and a reduced efficiency of the RF power amplifier. To reduce the PAPR, several techniques have been proposed which basically can be divided in three categories. First, there are signal distortion techniques, which reduce the peak amplitudes simply by nonlinearly distorting the OFDM signal at or around the peaks. Examples of distortion techniques are clipping, peak windowing, and peak cancellation [32] [33]. The second category is coding techniques that use a special forward-error correcting code set that exclude OFDM symbol with a large PAPR. The third technique is based on scrambling each OFDM symbol with different scrambling sequences and selecting the sequences that gives the smallest PAPR.

CHAPTER THREE

IQ IMBALANCE IN OFDM SYSTEMS

3.1 Introduction

In this chapter the OFDM receiver with front end analog impairments (such as IQ imbalance) is analyzed and description of the physical sources of IQ imbalances will be given. Based on the mathematical analysis an IQ imbalance model will be developed. In Section 3.3 effort is made to model the effects of IQ imbalance on OFDM systems in a form that will be exploited in subsequent chapters to drive compensation schemes for IQ imbalance.

3.2 IQ Imbalance model

The purpose of any receiver architecture is to convert a radio frequency (RF) signal down to the base band (BB). In the down-conversion, the RF signal is split over two paths, referred to as the I and Q component. Normally, the signal in the I component is down-converted by the Local Oscillator (LO) signal at the carrier frequency, while the Q component is down-converted by the LO signal with a 90° phase shift. The combination of these two signals results in the recovered baseband signal. Due to the physical characteristics of capacitors and resisters used to implement the analog components, the error in the nominal 90° phase shifts and imbalance between the amplitudes of the inphase(I)and quadirature phase (Q) signals will corrupt the downconverted signal constellation[43].

The imbalance between the amplitude of IQ channels and the phase shift errors is termed as the IQ imbalance [27] [40]. In order to develop a mathematical model for this imbalance, let us consider a black diagram of OFDM shown below.

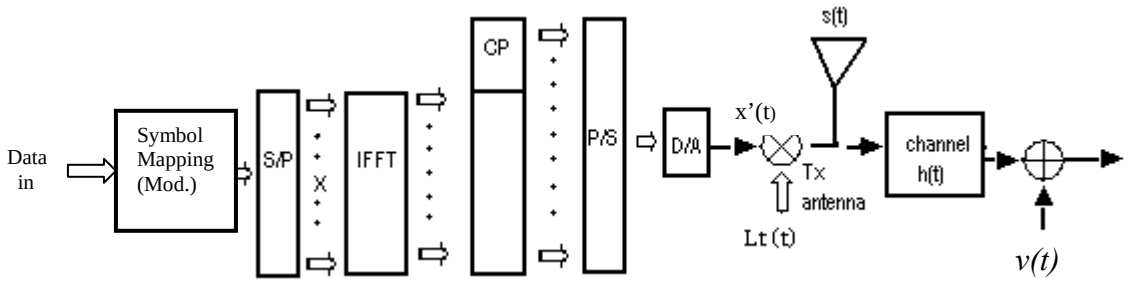

Figure 3.1a, OFDM transmitter block diagram

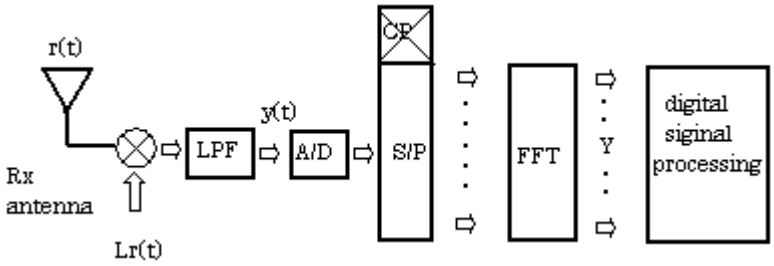

Figure 3.1b, OFDM receiver block diagram

Figure 3.1, OFDM system block diagram of direct-conversion architecture

As we can see from the figure 3.1, after passing the inverse fast Fourier transform block, the signal is converted to analog signal, $x'(t)$. Then, it is up converted by multiplication with the output of carrier signal source at the mixer. A carrier at transmitter is denoted by

$$L_t(t) = e^{-jw_c t} = e^{-j2\pi f t_c} \qquad (3.1)$$

Where $w_c = 2\pi f_c$ and carrier frequency is equal to f_c.

The impact of wireless communication channel can be modeled by the well known equivalent base band model [37], [39];

$$y(t) = x'(t) \otimes h(t) + v(t) \qquad (3.2)$$

Where '$\otimes$' is convolution operation and $h(t), v(t)$ denotes the complex valued baseband equivalents of the channel impulse response and channel noise respectively.

The real RF signal at the antenna of the receiver can be written as [39]

$$\begin{aligned} r(t) &= 2\,\mathrm{Re}\{y(t)e^{j2\pi f_c t}\} \\ &= y(t)e^{j2\pi f_c t} + y^*(t)e^{-j2\pi f_c t} \end{aligned} \qquad (3.3)$$

Where, y (t) denotes the complex baseband equivalent in the frequency band of interest

At the receiver, received signal is multiplied by receiver LO signal, $L_r(t)$ in order to down convert RF signal to the baseband. The principle of direct-conversion is to use a local oscillator (LO) with the frequency $f_{LO} = f_c$ and to apply complex (IQ) mixing.

For reference, we will first consider the case of no impairments (no IQ imbalance).In this case, the down-conversion yields the frequency band of interest

$$y(t) = Lp\{r(t)L_r(t)\} \tag{3.4}$$

Where $L_r(t) = e^{-j2\pi f_{LO}t}$ denotes the time function of the perfectly balanced complex LO and $Lp\{.\}$ denotes low pass filtering. If the direct-conversion architecture is used for the reception of an OFDM signal, $y(t)$ equals the received OFDM baseband signal. This signal is further A/D converted and its samples, $y(k)$, are used to compute the symbols on the sub carriers by applying the Discrete Fourier Transform (DFT).

Unfortunately, a perfect analog IQ mixing is not achievable in practice [42] [43]. In quadrature down conversion process, all the analog components such as mixer, phase-shifter, filters, in-phase and quadrature branches, and analog to digital converter (ADC) contribute to generate IQ imbalance. For convenience, the combined effects of all these imbalances are modeled as a quadrature mixing with an imbalanced LO signal as follows.

Let us denote the I and Q branch amplitudes by a_1 and a_2, and phases by θ_1 and θ_2 . The imbalanced LO signal $L_r'(t)$ can be expressed by,

$$L_r'(t) = a_1\cos(2\pi f_c t + \theta_1) - ja_2\sin(2\pi f_c t + \theta_2) \tag{3.5}$$

From mismatch points of view the imbalanced LO signal $L_r'(t)$ in (3.5) can be rearranged in a more convenient form as

$$L_r'(t) = a_1[\cos(2\pi f_c t + \theta_1) - j(a_2/a_1)\sin(2\pi f_c t + \theta_1 + (\theta_2 - \theta_1))]$$

To farther simplify the notation,

Let $a_1 = 1, \quad a_2 = a$ and

$\theta_1 = 0, \quad \theta_2 = \theta$

Hence, the imbalanced LO signal is expressed as

$$L_r'(t) = \cos(2\pi f_c t) - ja\sin(2\pi f_c t + \theta) \tag{3.6}$$

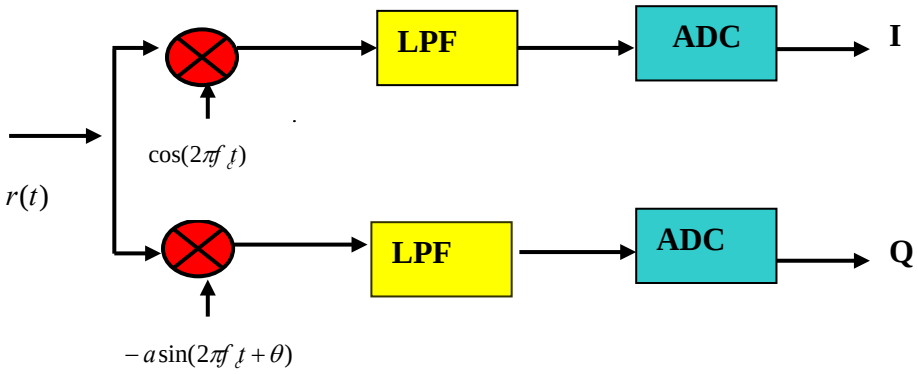

Figure 3.2, Imbalance model for analog front end processing

To understand the concepts of mismatch, equation (3.6) can be expressed in a more informative form. Hence, by applying Euler's formula to cosine and sine terms, $L_r'(t)$ in equation (3.6) can be expressed as;

$$L_r'(t) = \left[\frac{e^{j2\pi f_c t} + e^{-j2\pi f_c t}}{2}\right] - ja\left[\frac{e^{j(2\pi f_c t+\theta)} - e^{-j(2\pi f_c t+\theta)}}{2j}\right]$$

$$= \frac{(1+ae^{-j\theta})}{2}e^{-j2\pi f_c t} + \frac{(1-ae^{j\theta})}{2}e^{j2\pi f_c t}$$

$$= \alpha e^{-j2\pi f_c t} + \beta e^{j2\pi f_c t} \tag{3.7}$$

Where

$$\alpha = \frac{(1+ae^{-j\theta})}{2} \quad \text{and} \quad \beta = \frac{(1-ae^{j\theta})}{2} \tag{3.8}$$

In this case, the downconversion yields

$$y'(t) = Lp(r(t)L_r'(t))$$

$$= Lp\{[y(t)e^{j2\pi f_c t} + y*(t)e^{-j2\pi f_c t}].[\alpha e^{-j2\pi f_c t} + \beta e^{j2\pi f_c t}]\}$$

$$y'(t) = \alpha y(t) + \beta y^*(t) \qquad (3.9)$$

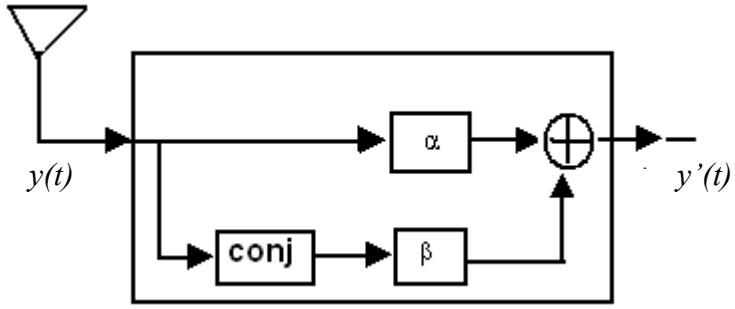

Figure 3.3, A time-domain model of IQ imbalance

This means, direct-conversion with IQ imbalance can be interpreted as a superposition of a desired complex down-conversion (weighted by α) and an undesired complex conjugate (weighted by β). Consequently, the received baseband signal with IQ imbalance $y'(t)$ is a superposition of the desired band limited signal $y(t)$ and it's conjugate $y*(t)$. This superposition translates to a mutual interference of symmetric OFDM symbol. This is clearly shown pictorially in the frequency-domain.

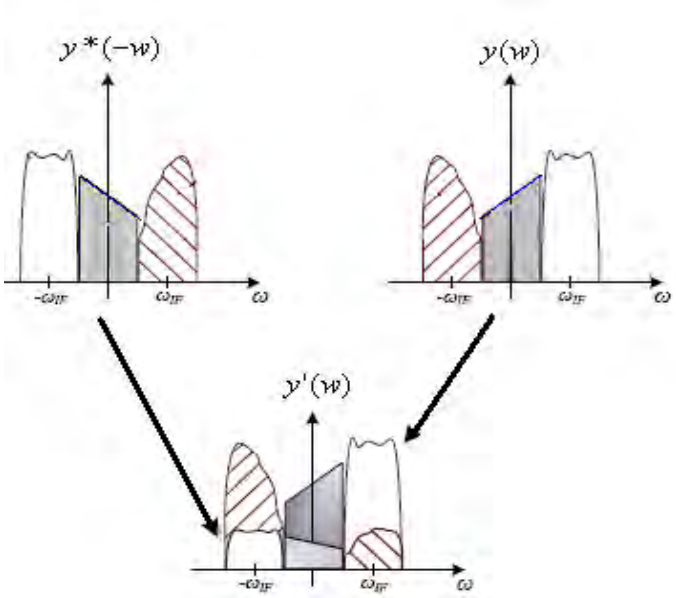

Figure 3.4, A frequency-domain illustration of the effects of IQ imbalance

3.3 Analysis of OFDM receivers with IQ imbalance

Let us consider a typical OFDM transmitter shown in figure 3.5. The input data stream is modulated by a QAM modulator, resulting in a complex symbols stream $X[0], X[1], \cdots, X[N-1]$. This symbol stream is passed through a serial-to-parallel converter, whose output is a set of N parallel QAM symbols $X[0], \ldots, X[N-1]$ corresponding to the symbols transmitted over each of the subcarriers. Thus, the N output symbols from the serial-to-parallel converter are the discrete frequency components of the OFDM modulator output $s(t)$. In order to generate $s(t)$, these frequency components are converted into time samples by performing an inverse DFT on these N symbols, which is efficiently implemented using the IFFT algorithm.

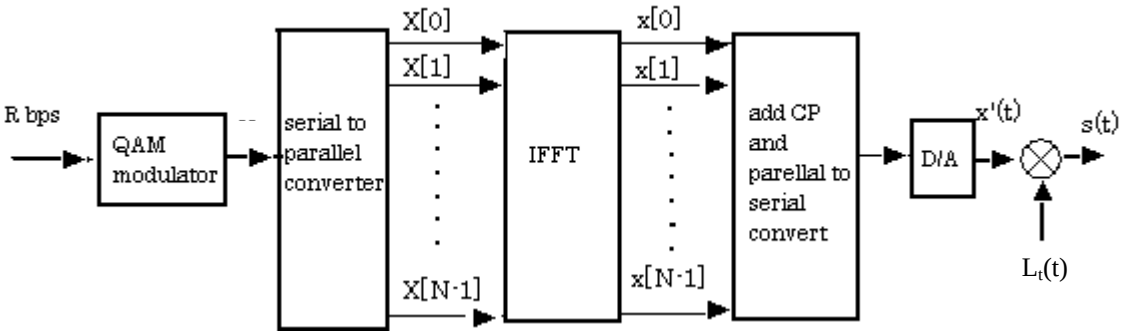

Figure 3.5, Typical OFDM transmitters

The IFFT yields the OFDM symbol consisting of the sequence x[n] = $x[0], \ldots, x[N-1]$ of length N,

Where x*[n]* is as described in equation (2.1) and it can be rewritten as

$$x[n] = \frac{1}{\sqrt{N}} \sum_{i=0}^{N-1} X[i] e^{j2\pi mi/N} \qquad 0 \le n \le N-1, \tag{3.10}$$

This sequence corresponds to samples of the multicarrier signal, i.e. the multicarrier signal consists of linearly modulated subchannels.

It is straightforward to show that the DFT operation on $x[n]$ can be represented by the matrix multiplication.

$$X = M\,x \tag{3.11}$$

where $X = (\,X[0], \ldots, X[N-1]\,)^T$, $x = (\,x[0], \ldots, x[N-1]\,)^T$, and M is an $N \times N$ matrix given by [44]

$$M = \frac{1}{\sqrt{N}} \begin{bmatrix} 1 & 1 & 1 & \cdots & 1 \\ 1 & W_N & W_N^2 & \cdots & W_N^{N-1} \\ \vdots & \vdots & \ddots & \vdots & \vdots \\ 1 & W_N^{N-1} & W_N^{2(N-1)} & \cdots & W_N^{(N-1)^2} \end{bmatrix} \tag{3.12}$$

$$W_N = e^{-j\frac{2\pi}{N}} \tag{3.13}$$

The cyclic prefix of length ε is then added to the OFDM symbol, and the resulting time samples $x'[n] = x'[-\varepsilon], \ldots\ldots, x'[N-1] = x[N-\varepsilon], \ldots x[0], \ldots x[N-1]$ are ordered by the parallel-to-serial converter and passed through a D/A converter, resulting in the baseband OFDM signal $x'(t)$, which is then up-converted to frequency f_c and transmitted as s(t) as shown in figure 3.5. By assuming at first that there is no IQ imbalance as shown in figure 3.6, The transmitted signal is filtered by the channel impulse response $h(t)$ and corrupted by additive noise, so that the received baseband equivalent of the frequency band of interest is, [39]

$$y(t) = x'(t) \otimes h(t) + v(t) \tag{3.14}$$

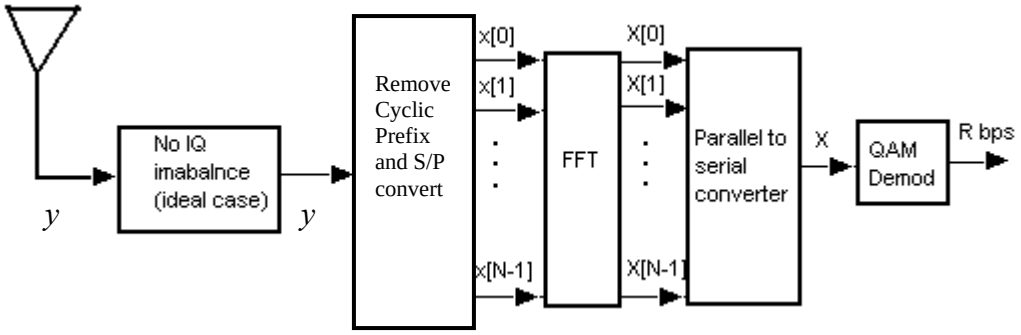

Figure 3.6, OFDM Receiver with Ideal IQ imbalance

This signal is downconverted to baseband and filtered to remove the high frequency components. The A/D converter samples the resulting signal to obtain

$$y[n] = x'[n] \otimes h[n] + v[n], \qquad -\varepsilon \le n \le N-1. \tag{3.15}$$

The prefix of $y[n]$ consisting of the first ε samples is then removed. Now let us consider a discrete-time channel with finite impulse response (FIR) as described in section (2.2.5) and as in [40] [45].

$$h[n] = h[0]..., h[\varepsilon] \text{ of length } \varepsilon + 1 = T_m/T_s \tag{3.16}$$

Where, T_m is the channel delay spread and T_s the sampling interval associated with the discrete time sequence. Denote also the nth element of these sequences as $h_n = h[n]$, $x'_n = x'[n]$, $v_n = v[n]$, and $y_n = y[n]$. With this notation the channel output sequence can be written as (2.2). In matrix form it can be rewritten as;

$$\begin{bmatrix} y_{N-1} \\ y_{N-2} \\ \vdots \\ y_0 \end{bmatrix} = \begin{bmatrix} h_0 & h_1 & \cdots & h_\varepsilon & 0 & \cdots & 0_{N+\varepsilon} \\ 0 & h_0 & \cdots & h_{\varepsilon-1} & h_\varepsilon & \cdots & 0 \\ \vdots & \vdots & \ddots & \ddots & \ddots & \ddots & \vdots \\ 0 & \cdots & 0 & h_0 & \cdots & h_{\varepsilon-1} & h_\varepsilon \end{bmatrix} \cdot \begin{bmatrix} x_{N-1} \\ \vdots \\ x_0 \\ x'_{-1} \\ \vdots \\ x'_{-\varepsilon} \end{bmatrix} + \begin{bmatrix} v_{N-1} \\ v_{N-2} \\ \vdots \\ v_0 \end{bmatrix} \tag{3.17}$$

The received symbols $y_{-1,\ldots,}y_{-\varepsilon}$ *are* discarded since they are affected by inter symbol interference (ISI) in the prior data block, and they are not needed to recover the input. The last ε symbols of $x[n]$ correspond to the cyclic prefix: $x'_{-1}=x_{N-1}, x'_{-2}=x_{N-2}, \cdots, x'_{-\varepsilon}=x_{N-\varepsilon}$. From this it can be shown that the matrix representation (3.17) is equivalent to the following representation [45].

$$\begin{bmatrix} y_{N-1} \\ y_{N-2} \\ \vdots \\ \vdots \\ \vdots \\ y_0 \end{bmatrix} = \begin{bmatrix} h_0 & h_1 & \cdots & h_\varepsilon & 0 & \cdots & 0_{N-1} \\ 0 & h_0 & \cdots & h_{\varepsilon-1} & h_\varepsilon & \cdots & 0 \\ \vdots & \vdots & \ddots & \ddots & \ddots & \ddots & \vdots \\ 0 & \dots & 0 & h_0 & \cdots & h_{\varepsilon-1} & h_\varepsilon \\ \vdots & \vdots & \ddots & \ddots & \ddots & \ddots & \vdots \\ h_2 & h_3 & \cdots & h_{\varepsilon-2} & \cdots & h_0 & h_1 \\ h_1 & h_2 & \cdots & h_{\varepsilon-1} & \cdots & 0 & h_0 \end{bmatrix} \begin{bmatrix} x_{N-1} \\ x_{N-2} \\ \vdots \\ \vdots \\ x_0 \end{bmatrix} + \begin{bmatrix} v_{N-1} \\ v_{N-2} \\ \vdots \\ \vdots \\ \vdots \\ v_0 \end{bmatrix}$$

(3.18)

This can be rewritten compactly as,

$$y = Hx + v \qquad \textit{(3.19)}$$

This equivalent model shows that the inserted cyclic prefix allows the channel to be modeled as a circulant convolution matrix H over the *N* samples of interest.

The matrix H is $N \times N$, so it has an eigenvalue decomposition [45],

$$H = M^* \Lambda M \qquad (3.20)$$

Where Λ is a diagonal matrix of eigenvalues of H and M *is* a unitary matrix whose rows comprise the eigenvectors of H. i.e. $\lambda_i \mathbf{m}_i = \mathrm{H}\mathbf{m}_i$ for $i = 0, 1, \ldots, N-1$, where $\mathbf{m}_i$ denotes the i_{th} row of M. Hence,

$$H = M^* diag(\lambda) M \qquad (3.21)$$

The vector λ is related to channel tap, $h' = [h_0, h_1, ..., h_\varepsilon]^T$ via [36] [40]

$$\lambda = \sqrt{N} M^* \begin{bmatrix} h' \\ 0_{(N-(\varepsilon+1))\times 1} \end{bmatrix} \qquad (3.22)$$

Thus, if we insert equation (3.21) in equation (3.19), we can rewrite equation (3.19) as;

$$y = M^{*}\Lambda M\, x + v$$
$$= M * diag(\lambda) M\, x + v \qquad (3.23)$$

Then y is passed to a serial to parallel converter and then demodulated with FFT as shown in figure 3.6.

Now, let us consider the case where the received data is distorted by IQ imbalance as shown in figure 3.7. The received block of data y' after being distorted by IQ imbalances becomes

$$y' = \alpha\, y + \beta\, conj(y) \qquad (3.24)$$

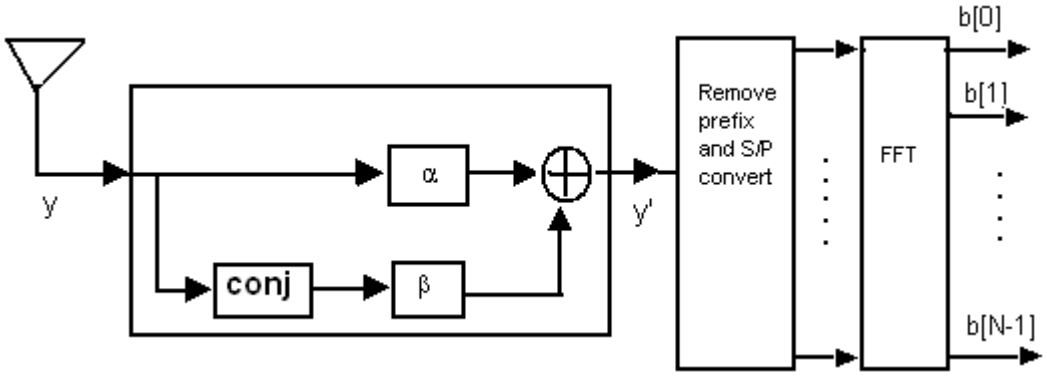

Figure 3.7, OFDM receivers with IQ imbalance

$$conj(y) = conj(Hx + v) = conj(H)conj(x) + conj(v)$$

But from [36] we know that

$$conj(H) = M^{*} diag(\lambda') M \qquad (3.25)$$

Where,

$$\lambda' = \sqrt{N} M^{*} \begin{bmatrix} conj\ (h') \\ 0_{(N-(\varepsilon+1))x1} \end{bmatrix} \qquad (3.26)$$

Thus,

$$conj[y] = M^{*} diag(\lambda') M\ conj(x) + conj(v) \tag{3.27}$$

Now, let us substitute equation (3.23) and (3.27) in equation (3.24)

$$y' = \alpha[M^{*} diag(\lambda) M\ x + v] + \beta[M^{*} diag(\lambda') M\ conj(x) + conj(v)]$$

After it passes through a serial to parallel converter and then through FFT it becomes,

$$b = \alpha\, diag(\lambda)\, X + \beta\, diag(\lambda')\, X' + v' \tag{3.28}$$

Where $b = My', X = Mx, X' = Mconj(x)$ and v' is a transformation version of original noise v

We know from the properties of DFT [42] [45] that, for $1 \le n \le N$ and $1 \le k \le N$

$$If, X = Mx = \begin{bmatrix} X(1) \\ X(2) \\ \vdots \\ X(\frac{N}{2}) \\ X(\frac{N}{2}+1) \\ X(\frac{N}{2}+2) \\ \vdots \\ X(N) \end{bmatrix} \quad \text{then} \quad X' = Mconj(x) = \begin{bmatrix} X^{*}(1) \\ X^{*}(N) \\ \vdots \\ X^{*}(\frac{N}{2}+2) \\ X^{*}(\frac{N}{2}+1) \\ X^{*}(\frac{N}{2}) \\ \vdots \\ X^{*}(2) \end{bmatrix} \tag{3.29}$$

We substitute equation (3.29) in equation (3.28) and for simplicity of presentation, we discard the samples corresponding to tones 1 and N/2 + 1, i.e. b (1) and b (N/2 + 1).

The reason for discarding these two samples is that the transformation (3.29) returns the same indices only for i = 1 and $i = N/2 + 1$ and mirrors and conjugates all other tones. In other words, in (3.29), $X(1)$ and $X(\frac{N}{2}+1)$ become $X^{*}(1)$ and $X^{*}(\frac{N}{2}+1)$, respectively, without any change in their indices. For all other tones, their indices become mirrored around the tone $N/2 + 1$. In

order to have a unified formulation for all the tones, these two tones are discarded. However, if desired, a set of equations can be derived specifically for the tones 1 and *N*/2 + 1 in a manner similar to (3.33)-(3.35). Note that in standardized OFDM systems such as IEEE 802.11a [14] these two tones do not carry any information due to implementation issues. Sending zeros on these two tones relaxes the implementation requirements on the receiver analog filters and DC offset as shown in section (2.2.3).

Define two new vectors:

$$X'' = [X(2),.....,X(N/2),X^*(N/2+2),.....,X^*(N)]^T$$

and

$$B = [b(2),.....,b(N/2),b^*(N/2+2),.....,b^*(N)]^T \tag{3.30}$$

Then, equation (3.28) became,

$$B = WX'' + V'' \tag{3.31}$$

Where

$$W = \begin{bmatrix} \alpha\lambda(2) & & & & & & \beta\lambda^*(N) \\ & \ddots & & & & \iddots & \\ & & \alpha\lambda(\frac{N}{2}-1) & 0 & 0 & \beta\lambda^*(\frac{N}{2}+3) & \\ & & & \alpha\lambda(\frac{N}{2}) & \beta\lambda^*(\frac{N}{2}+2) & & \\ & & & \beta^*\lambda(\frac{N}{2}) & \alpha^*\lambda^*(\frac{N}{2}+2) & & \\ & & \beta^*\lambda(\frac{N}{2}-1) & 0 & 0 & \alpha^*\lambda^*(\frac{N}{2}+3) & \\ & \iddots & & & & \ddots & \\ \beta^*\lambda(2) & & & & & & \alpha^*\lambda^*(N) \end{bmatrix} \tag{3.32}$$

Where V'' is related to v' in a manner similar to (3.30).

The elements in the second halves of X'' and B are conjugated due to the structure of equation (3.28). As we can see from (3.28), the vector b is no longer related to the transmitted block X through a diagonal matrix, as is the case in an OFDM system with ideal I and Q branches. We can also clearly see that matrix W can be reduced to diagonal matrix if we let β=0 which is equal to the ideal case.The objective is now to recover the signal X'' from the received signal B in equation (3.31) or alternatively, we can rewrite equation (3.31) as follows,

For $i = 2,\cdots\frac{N}{2}$

$$\begin{bmatrix} b(i) \\ b^*(N-i+2) \end{bmatrix} = \begin{bmatrix} \alpha\lambda(i) & \beta\lambda^*(N-i+2) \\ \beta^*\lambda(i) & \alpha^*\lambda^*(N-i+2) \end{bmatrix} \cdot \begin{bmatrix} X(i) \\ X^*(N-i+2] \end{bmatrix} + \begin{bmatrix} v(i) \\ v^*(N-i+2) \end{bmatrix} \tag{3.33}$$

$$b_i = A_i X_i + v_i \tag{3.34}$$

Where

$$b_i = \begin{bmatrix} b(i) \\ b^*(N-i+2 \end{bmatrix},\ A_i = \begin{bmatrix} \alpha\lambda(i) & \beta\lambda^*(N-i+2) \\ \beta^*\lambda(i) & \alpha^*\lambda^*(N-i+2) \end{bmatrix} \text{ and } v_i = \begin{bmatrix} v(i) \\ v^*(N-i+2) \end{bmatrix} \tag{3.35}$$

The objective here is to recover $X(i)$ and $X^*(N-i+2)$ from received signal $b(i)$ and $b^*(N-i+2)$ as it is going to be shown on the next chapter

CHAPTER FOUR

OFDM RECEIVERS WITH COMPENSATION FOR IQ IMBALANCES

4.1 Introduction

In the previous chapter, we have modeled the impact of IQ imbalance on OFDM based Systems. Now in this chapter, we develop compensation algorithms in the digital domain using the models developed in chapter three. The algorithms include least square (LS) compensation, as well as an adaptive compensation scheme with improved convergence rate. All compensation schemes use training to estimate the distortion parameters that model the IQ imbalances. For systems such as IEEE 802.11a and IEEE 802.11g that feature a dedicated pilot sequence, the same training data used for channel estimation in standard OFDM systems can be used for joint channel and distortion estimation. For systems that do not provide dedicated training symbols, a decision directed scheme can be used.

4.2 Least-Square Compensation

Consider equation (3.34). Because of the noise component v_i the observed vector b_i does not lie in the column space of the matrix A_i. The objective of the least-squares problem is to determine the vector in the column space of A_i that is closet to b_i in the least-squares sense. It is therefore desired to determine the particular $\hat{X}_i$ that minimizes the distance between b_i *and* $A_i\hat{X}_i$

$$\min_{X_i} \| b_i - A\hat{X}_i \|^2 \qquad (4.1)$$

The resulting $\hat{X}_i$ is called the least-square solution and it provides an estimate for the unknown X_i. $A_i\hat{X}_i$ is called the least-squares estimate of b_i.

The solution to (4.1) exists and it follows from a simple geometric argument. The orthogonal projection of b_i onto the column span of A_i yields a vector $A_i\hat{X}_i$ that is the closest to b_i in the least square sense. This is because the resulting error vector ($b_i - A_i\hat{X}_i$) will be orthogonal to the column span of A.

In other words, the closest element $A_i\hat{X}_i$ to b_i must satisfy the orthogonality condition,

$$A_i^T \cdot (b_i - A_i \cdot \hat{X}_i) = 0 \qquad (4.2)$$

Therefore, the least-squares estimate of $X(i)$ *and* $X^*(N-i+2)$ *for* $i = 2,...,\frac{N}{2}$, denoted by $\hat{X}(i)$ and $\hat{X}(N-i+2)$, are given by

$$\Rightarrow \quad \hat{X}_i = (A_i^T \cdot A_i)^{-1} \cdot A_i^T \cdot b_i \qquad (4.3)$$

Now, in order to get the solution for equation (4.3), the channel information λ and the distortion parameters (α *and* β) are required. Training symbols can be used to enable the receiver to estimate those values. Thus note that we may use equation (3.33) for channel estimation purposes by rewriting it as:

for $i = 2,...\frac{N}{2}$

$$\begin{bmatrix} b(i) \\ b^*(N-i+2) \end{bmatrix} = \begin{bmatrix} X(i) & 0 & X^*(N-i+2) & 0 \\ 0 & X(i) & 0 & X^*(N-i+2) \end{bmatrix} \cdot \begin{bmatrix} \alpha\lambda(i) \\ \beta^*\lambda(i) \\ \beta\lambda^*(N-i+2) \\ \alpha^*\lambda^*(N-i+2) \end{bmatrix} + \begin{bmatrix} v(i) \\ v^*(N-i+2 \end{bmatrix} \qquad (4.4)$$

$$let \quad \Theta_i = \begin{bmatrix} X(i) & 0 & X^*(N-i+2) & 0 \\ 0 & X(i) & 0 & X^*(N-i+2) \end{bmatrix} \text{ and } \Psi_i = \begin{bmatrix} \alpha\lambda(i) \\ \beta^*\lambda(i) \\ \beta\lambda^*(N-i+2) \\ \alpha^*\lambda^*(N-i+2) \end{bmatrix} \qquad (4.5)$$

$$b_i = \Theta_i \Psi_i \quad + \quad v_i \qquad (4.6)$$

The least mean-square estimate of joint channel and IQ parameter can be found from equation (4.6) as

$$\hat{\Psi}_i = \Theta_i^T (\Theta_i . \Theta_i^T)^{-1} b_i \qquad (4.7)$$

Where, superscript ^{T} stands for transpose of a matrix. Note also that b_i and v_i as defined in (3.35).

Assuming *n* OFDM symbols are transmitted for training, and then *n realizations* of the equation (4.7) can be collected to perform the least-squares estimation of the elements forming A_i i.e. channel taps $\lambda(i)$ *and* $\lambda^*(N-i+2)$ and the distortion parameters α *and* β. The estimated A_i can then be substituted in (4.3) for data estimation.

The same training data used for channel estimation in standard OFDM systems such as IEEE802.11a and IEEE802.11g can be used in this scheme for the joint estimation of channel and distortion parameters. For systems that do not provide dedicated training symbols, a decision directed scheme could be used where the recovered data at the receiver are used for training. In this case, a low density constellation (e.g., QPSK) could be used during the initial transmission phase since errors due to IQ imbalances are less severe for low density constellations. The estimator (4.3) is optimal in the least-squares sense and will be referred to as least-squares equalization.

The resulting receiver structure is shown as follows.

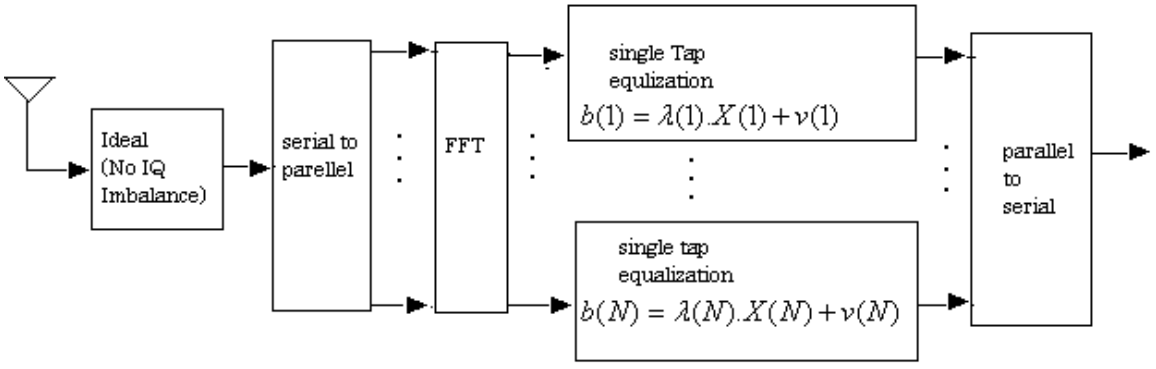

Figure 4.1, Standard OFDM receivers assuming ideal IQ branches

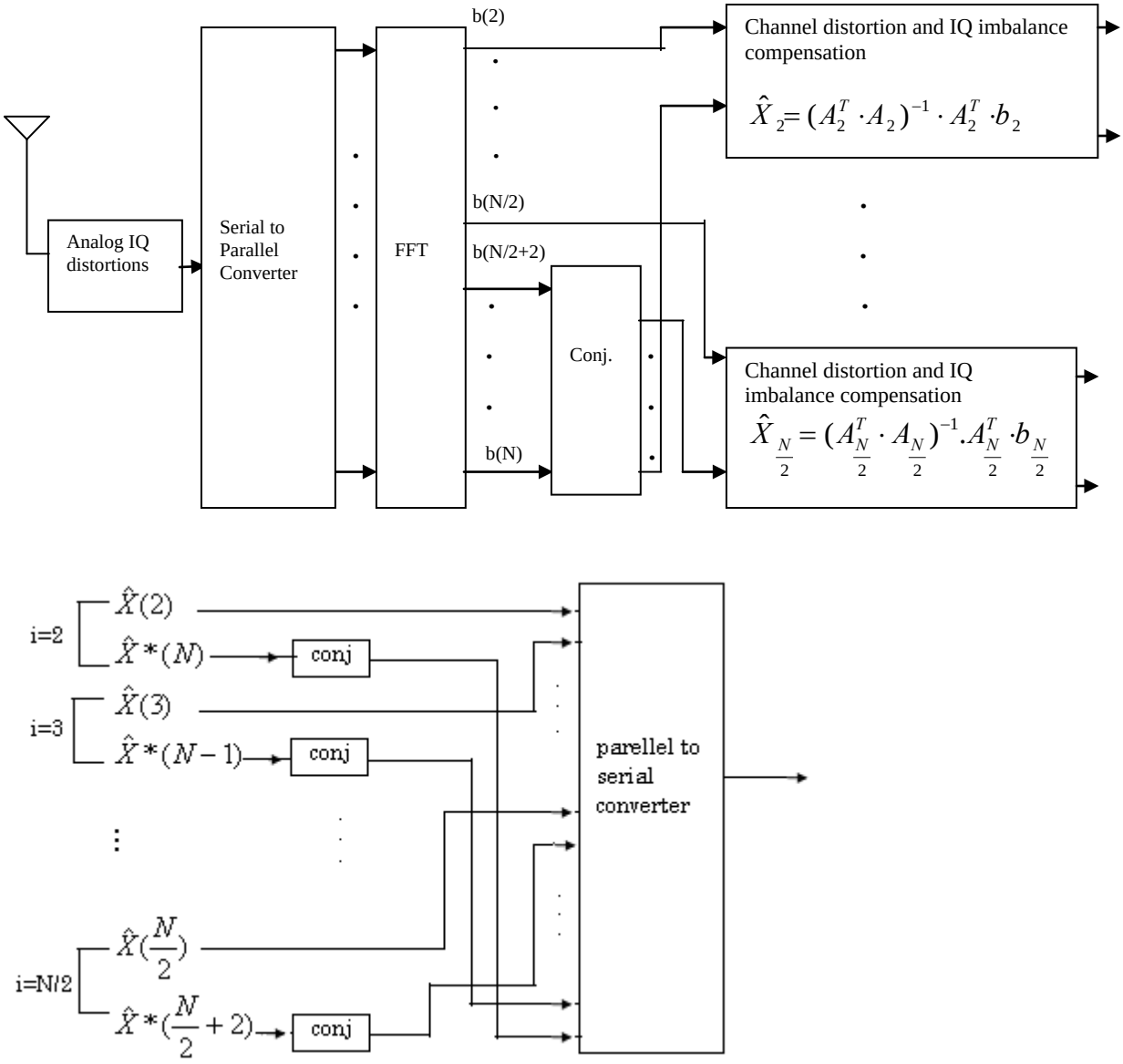

Figure 4.2, OFDM receivers with least square compensation of IQ imbalance

4.3 Adaptive Compensation

The least mean square (LMS) algorithm is a popular adaptive algorithm because of its simplicity and robustness. The LMS estimation of $X(i)$ *and* $X^*(N-i+2)$ in (1.33) can be attained as follows:

$$\hat{X}(i) = w_i \cdot \begin{bmatrix} b(i) \\ b^*(N-i+2) \end{bmatrix} \qquad (4.8)$$

$$\hat{X}^*(N-i+2) = w_{N-i+2} \cdot \begin{bmatrix} b(i) \\ b^*(N-i+2) \end{bmatrix} \tag{4.9}$$

Where w_i *and* w_{N-i+2} are (1×2) equalization vectors updated according to LMS algorithms for $i = 2,\cdots,\frac{N}{2}$.

To better illustrate the update equations, we introduce a time (or iteration) index *k*. Thus, let ${w_i}^k$ *and* ${w^k}_{N-i+2}$ represent the equalization terms at time instant *k*. Furthermore, let $b^k(i)$ *and* $b^{*k}(N-i+2)$ represent the term $b(i)$ *and* $b^*(N-i+2)$ at the same time instant *k*. Now, the equalization coefficients for *i* =2,...,*N/2* are updated according to the LMS rules[45]:

$$w_i^{(k+1)} = {w_i}^{(k)} + \mu_{LMS} \cdot \begin{bmatrix} b^{(k)}(i) \\ b^{*(k)}(N-i+2) \end{bmatrix}^H \cdot e_i^{(k)} \tag{4.10}$$

$$w_{N-i+2}^{(k+1)} = w_{N-i+2}^{(k)} + \mu_{LMS} \cdot \begin{bmatrix} b^{(k)}(i) \\ b^{*(k)}(N-i+2) \end{bmatrix}^H \cdot e_{N-i+2}^{(k)} \tag{4.11}$$

Where ^{H} stands for conjugate transpose of a matrix. The LMS algorithm converges in the mean if $0 < \mu_{LMS} < \frac{2}{\lambda_{\max}}$.

Where μ_{LMS} is the step-size parameter and $\lambda_{\max}$ is the maximum eigenvalue of the autocorrelation matrix R_b [45].

The error signal generated at iteration k for the tone index i using a training symbol $d_i^{(k)}$ are expressed as

$$e_i^{(k)} = d_i^{(k)} - w_i^{(k)} \cdot \begin{bmatrix} b^{(k)}(i) \\ b^{*(k)}(N-i+2) \end{bmatrix} \tag{4.12}$$

$$e_{N-i+2}^{(k)} = d_{N-i+2}^{(k)} - w_{N-i+2}^{(k)} \cdot \begin{bmatrix} b^{(k)}(i) \\ b^{*(k)}(N-i+2) \end{bmatrix} \tag{4.13}$$

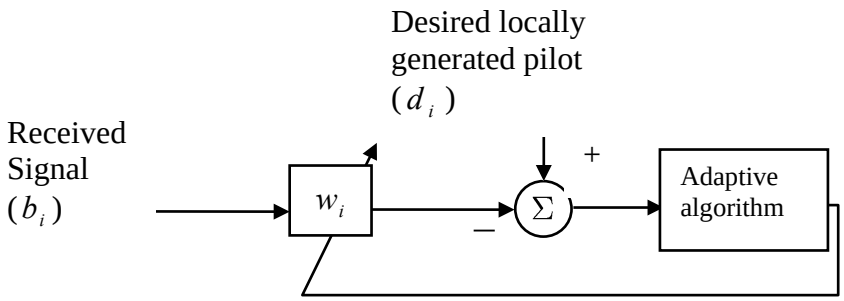

Figure 4.3, Adaptive compensation techniques

During training mode, a known pilot signal is sent over the channel and is received as received signal (b_i). At the receiving end, the pilot signal is locally generated and used in the adaptation algorithm as shown in figure 4.3

The LMS algorithm is most commonly used adaptive algorithm because of its simplicity and a reasonable performance. Since it is an iterative algorithm it can be used in a highly time-varying signal environment. It has a stable and robust performance against different signal conditions. However it may not have a really fast convergence speed [45][46].This problem is severe for the application at hand, since current OFDM systems usually deploy a short training sequence in order to reduce training overhead in packet-based data transmission.

A short training length is acceptable due to the fact that an OFDM system with ideal I and Q branches can achieve good channel estimation with only a few training symbols. However, in the presence of IQ imbalances, there is cross coupling between every tone and its conjugate tone, which makes the convergence rate slower. In LMS, the coefficients in (4.8 and 4.9) are usually initiated with zero as their initial values. In order to improve the convergence rate of the algorithm significantly, the equalizer coefficients are initialized to values calculated by assuming ideal I and Q branches.

Consider equation (3.33), for ideal case, we set $\alpha = 1 \; and \; \beta = 0$. In this situation, equation (3.33) becomes,

for $i = 2, \cdots, \frac{N}{2}$

$$\begin{bmatrix} b(i) \\ b^*(N-i+2) \end{bmatrix} = \begin{bmatrix} \lambda(i) & 0 \\ 0 & \lambda^*(N-i+2) \end{bmatrix} \cdot \begin{bmatrix} X(i) \\ X^*(N-i+2] \end{bmatrix} + \begin{bmatrix} v(i) \\ v^*(N-i+2) \end{bmatrix} \quad (4.14)$$

If we use the first n OFDM symbols for training, then the least square estimate for channel is given by

$$\hat{\lambda}(i) = \frac{\sum_{k=1}^{n} X_k^*(i) b_k(i)}{\sum_{k=1}^{n} X_k^*(i) X_k(i)} \quad (4.15)$$

Where $X_k(i)$ *and* $b_k(i)$ denote the transmitted and received *ith* tones at time instant k

Similarly,

$$\hat{\lambda}^*(N-i+2) = \frac{\sum_{k=1}^{n} X_k(N-i+2) b_k{}^*(N-i+2)}{\sum_{k=1}^{n} X_k(N-i+2) X_k{}^*(N-i+2)} \quad (4.16)$$

Using the above estimation for channel parameter, the 2×1 equalization vectors w_i *and* $w_{(N-i+2)}$ in equation (4.8 and 4.9) are initialized to

$$w_i^{(0)} = \begin{bmatrix} \frac{1}{\hat{\lambda}(i)} & 0 \end{bmatrix} \quad \text{and} \quad w_{N-i+2}^{(0)} = \begin{bmatrix} 0 & \frac{1}{\hat{\lambda}^*(N-i+2)} \end{bmatrix} \quad (4.17)$$

These initial values are closer to the final value when compared to an all zero initialization, since the parameter β in (3.35) is typically much smaller than the α parameter. By using these as initial value for estimation, we can get fast converged result than that of using zero as initial value for estimation. This is also verified using the computer simulation. In order to verify this, the error is set to 0.002 and the average number of iteration need for both case i.e. for case of initial set to zero and for case of initial set to ideal IQ are counted and it is seen that the average number of iteration needed if we set the initial values to ideal IQ is reduced by half than using zero as initial value.

CHAPTER FIVE

SIMULATION AND RESULTS

In many packet transmission systems, such as wireless LAN, the packet length is short enough to assume a constant channel conditions during the length of the packet. This means there is no need to estimate time fading, which greatly simplifies the channel and IQ distortion estimation problems. If we use a pilots scattered over several OFDM data symbols, it introduce a delay of several symbols before the first channel and distortion estimate can be calculated. Such a delay is undesirable in packet transmission like in an IEEE 802.11 wireless LAN, which requires an acknowledgment to be sent after each packet transmission. Any delay in the reception of packet will also delay the acknowledgments and hence decrease the effective throughput of the system. An additional disadvantage is the fact that the receiver needs to buffer several OFDM symbols, thereby requiring extra hardware.

For our specific problem of channel and IQ distortion estimation, the most appropriate approach seems to be the use of training consists of one or more known OFDM symbols. This approach is sketched in figure 5.1. The figure shows the time frequency grid with subcarrier on the vertical axis and symbols on the horizontal axis. This block type pilot arrangement is used during the simulation.

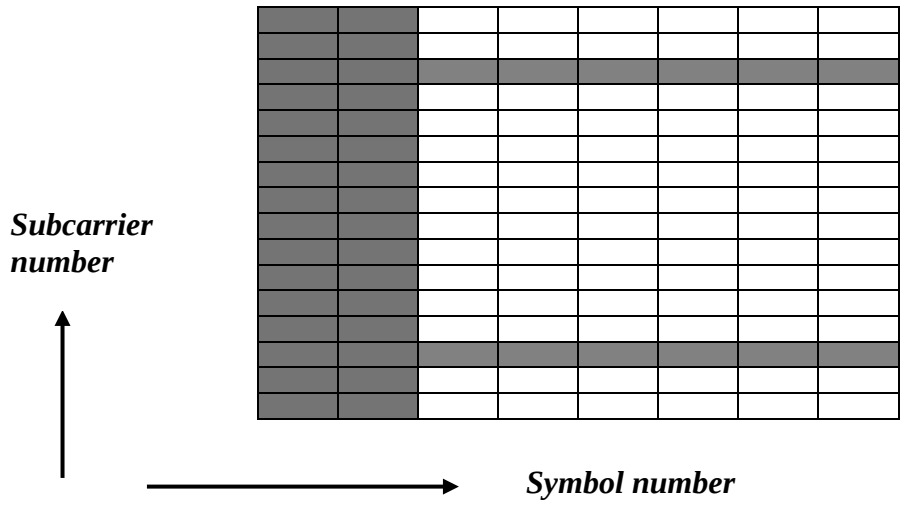

Figure 5.1, Examples of a packet with two training symbols for channel and IQ parameter estimation and two pilots subcarriers used for frequency synchronization.

The packet starts with two OFDM symbols for all data value are known. These training symbols can be used to obtain channel and IQ parameter estimates as well as frequency offset estimates. After the first two training symbols, figure 5.1 shows the two pilot subcarriers within the data symbols. These pilots are not meant for channel estimation, but for tracking the remaining frequency offset after the initial training. This is because frequency offset affects all the subcarries in a similar way as shown in equation (2.13) hence there is no need to have many pilots with small frequency spacing as in the case of channel and IQ estimation.

The choice of the number of training symbols is a tradeoff between a short training time and a good channel and IQ parameter estimation performance. One of the main assumptions when using pilot symbols only at the start of the packet is that channel variations during the rest of the packet are negligible. Whether this is a valid assumption depends on the packet durations and the Doppler bandwidth.

The choice of various OFDM parameters is a tradeoff between various requirements. Usually, there are three main requirements to start with: Bandwidth, bit rate, and delay spread. The delay spread directly dictates the guard time. Usually, the guard time is chosen about two to four times the roots mean squared delay spread [51]. This value depends on the type of coding and QAM modulation. Higher order QAM (like 64-QAM) is more sensitive to ICI and ISI than QPSK while heavier coding obviously reduces the sensitivity to such interference [51].

Now that the guard time has been set, the symbol duration can be fixed. To minimize the signal to noise ratio (SNR) loss caused by the guard time, it is desirable to have the symbol duration much larger than the guard time. It can’t arbitrarily be large, however, because a large symbol duration means more subcarries with a smaller subcarrier spacing, which result in a larger implementation complexity, and more sensitivity to phase noise and frequency offset [47], as well as increased peak-to average power ratio[48][49]. Hence a practical design choice is to make the symbol duration at least five times the guard time [51].

After the symbol duration and guard time are fixed, the number of subcarriers may be determined by the required bit rate divided by the bit rate per subcarrier. The bit rate per subcarrier is defined by the modulation type (e.g. 16 QAM), coding rate, and symbol rate.

Based on the above discussion, in our simulation the following parameters are assumed

- Bit rate 20Mbps
- Tolerable delay spread 200ns
- Bandwidth $\leq$ 20MHZ

The delay spread requirement of 200 ns suggests that 4 times the delay spread (800ns) is safe value for the guard time. The OFDM symbol duration is assumed 5 times the guard time i.e. 4 μs. To determine the number of subcarriers needed, we look at the ratio of the required bit rate and OFDM symbol rate. To do this there are several options. However in our simulation we use uncoded 16QAM and 64QAM.

- Number of FFT points 64
- The cyclic prefix length of 16
- The channel length (ε+1 = 4). The channel taps are chosen independently with complex Gaussian distribution.

The BER versus SNR for the presented schemes are simulated and shown in Figures 5.2-5.6. In all figures, the “Ideal IQ” legend refers to a receiver with no IQ imbalance and perfect channel knowledge and the “IQ imbalance without Compensation” Legend refers to a receiver with IQ imbalance but no compensation scheme. Moreover, the legends “with LS compensation” and “with LMS compensation” refer to the schemes presented in chapter four Sections 4.2 and 4.3 respectively. The results are depicted for different constellation sizes and different length of training sequences. Note also that Figure 5.7 shows the system performances as phase imbalances increases from 0-5 degree by keeping amplitude imbalances at 1dB and SNR at 20dB constant.

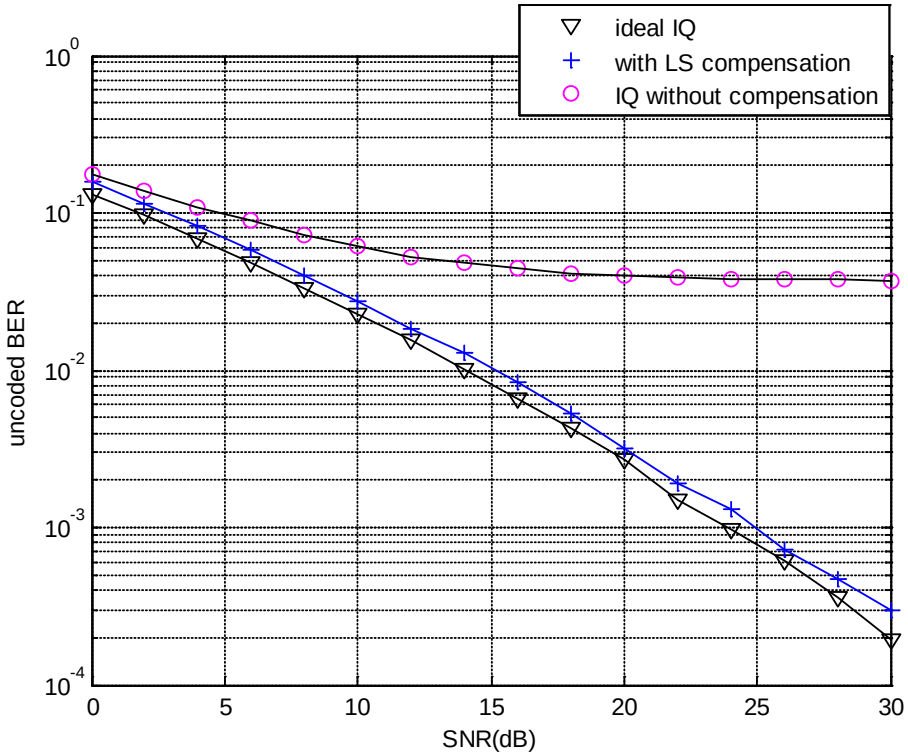

Figure 5.2, BER vs. SNR simulated for 16QAM constellation, phase imbalance of 2°, amplitude imbalance of 1dB, and training length of 5 OFDM symbols.

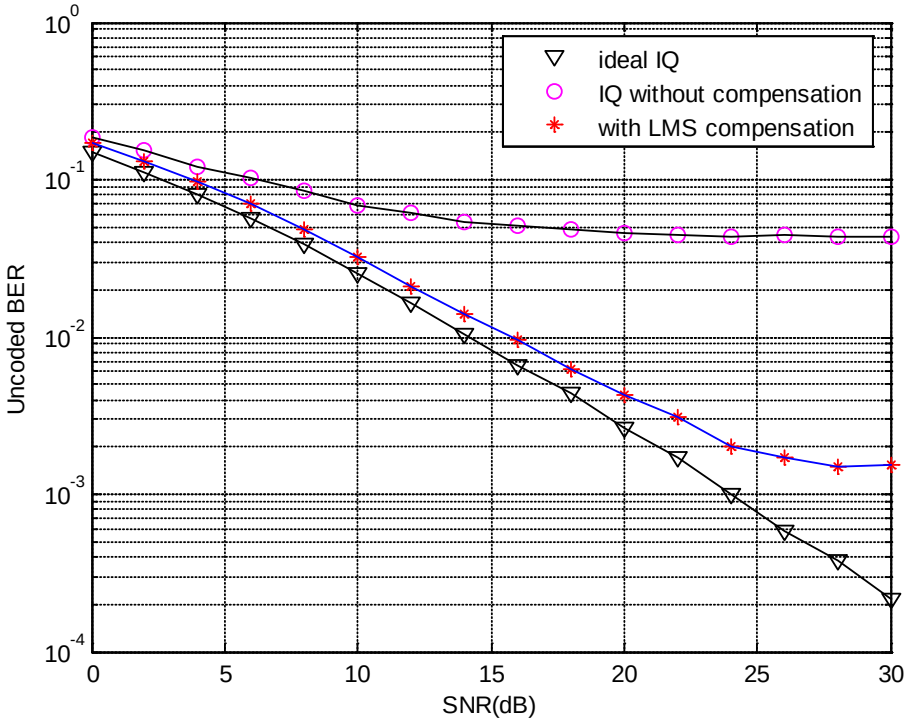

Figure 5.3, BER vs. SNR simulated for 16QAM constellation, phase imbalance of 2°, amplitude imbalance of 1dB, step size parameter $\mu_{LMS}= 0.2$ and training length of 20 OFDM symbols.

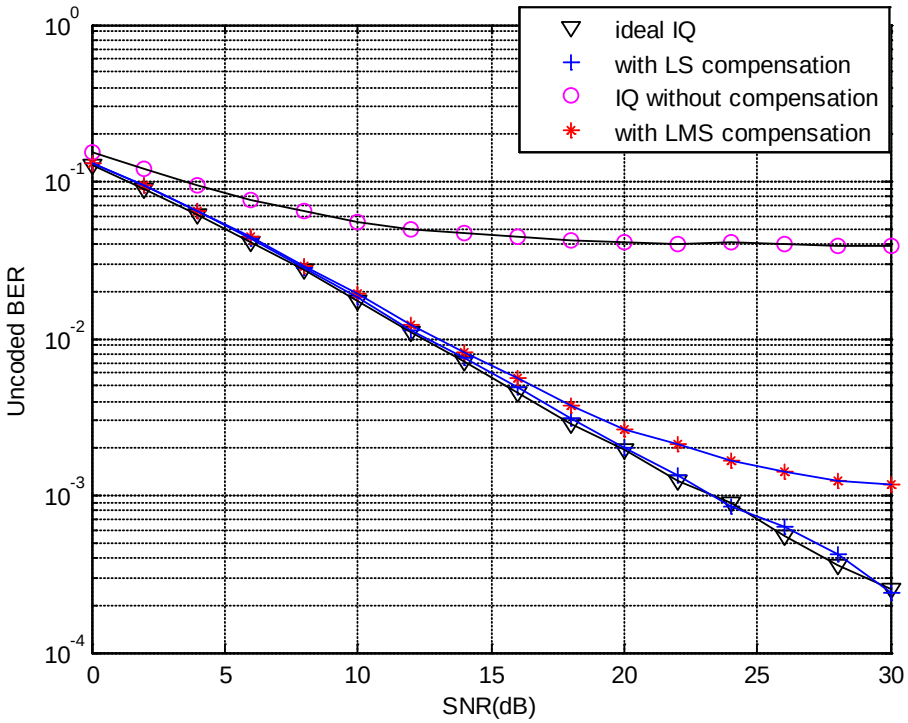

Figure 5.4, BER vs. SNR simulated for 16QAM constellation, phase imbalance of 2°, amplitude imbalance of 1dB, step size parameter $\mu_{LMS}= 0.2$ and training length of 25 OFDM symbols.

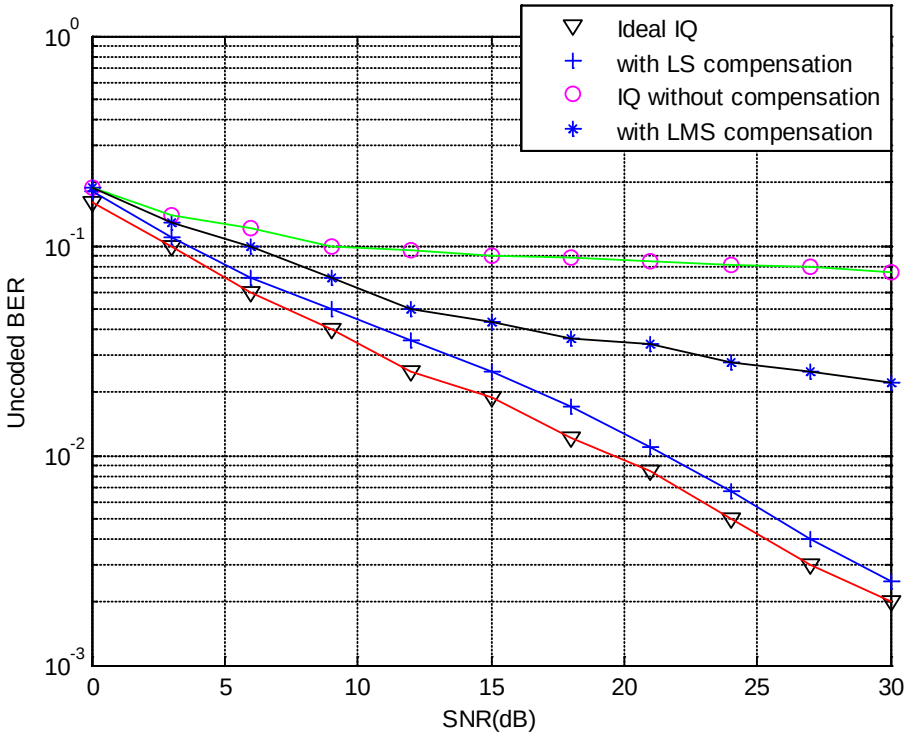

Figure 5.5, BER vs. SNR simulated for 64QAM constellation, phase imbalance of 2°, amplitude imbalance of 1dB, step size parameter $\mu_{LMS}= 0.2$ and training length of 10 OFDM symbols.

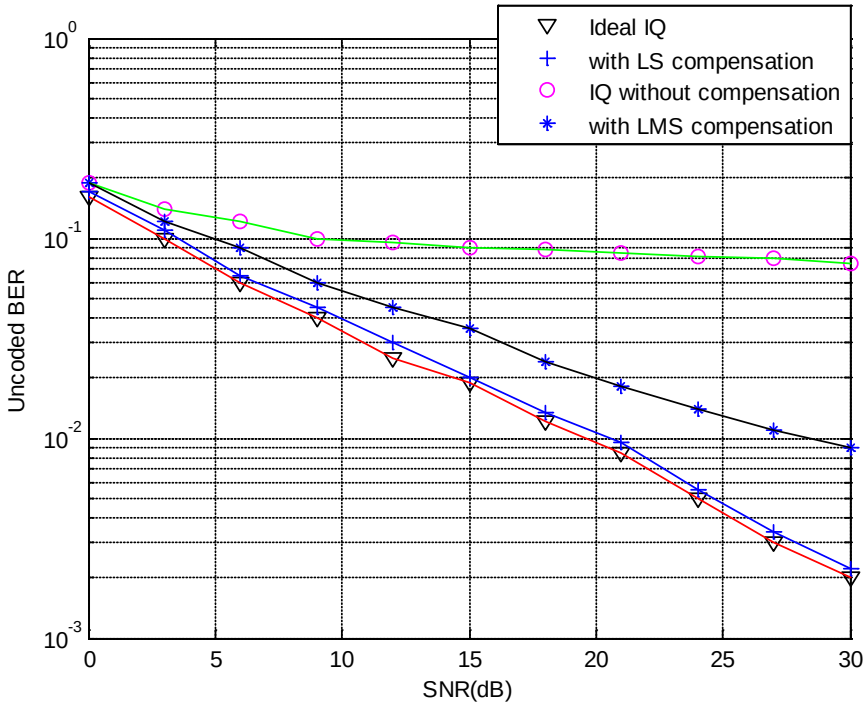

Figure 5.6, BER vs. SNR simulated for 64QAM constellation, phase imbalance of 2°, amplitude imbalance of 1dB, step size parameter $\mu_{LMS}= 0.2$ and training length of 25 OFDM symbols.

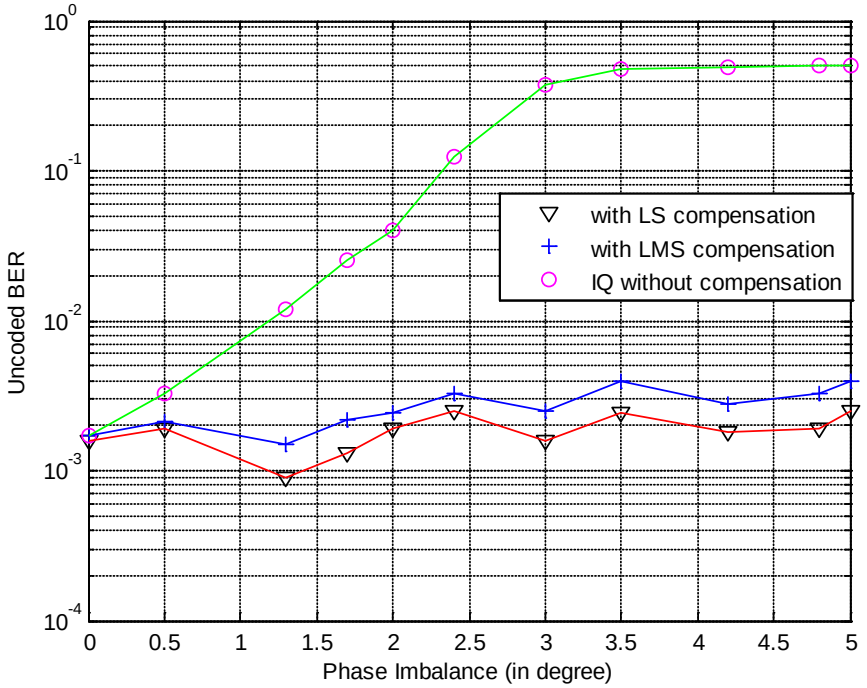

Figure 5.7, BER vs. phase imbalance (in degree) simulated for 16QAM constellation, amplitude imbalance of 1dB, SNR kept constant at 20dB, phase imbalance varies from $0-5^{\circ}$, step size parameter $\mu_{LMS}= 0.2$ and training length of 25 OFDM symbols.

As can be seen in all simulation results, the degradation in the BER values due to IQ imbalances is significant. Figures 5.2-5.6 show the simulation results for typical (practical) distortion parameter values; phase imbalance of 2° and gain imbalances 1dB. An important observation is that the BER curves become saturated in the presence of IQ imbalances. In other words, even increasing the operating SNR does not help improve the BER values, emphasizing the need for digital compensation schemes.

It is seen that least-squares algorithms perform close to the ideal case. The simulation results also show that the performance of the adaptive compensation scheme depends on the length of the available training sequence. Decision directed approach can be used to provide many number of training symbols in real scenarios. From figure 5.7 we can clearly see that also for large phase imbalance, the proposed compensation strategy works quit satisfactory.

CHAPTER SIX

CONCLUSION AND FUTURE WORK

6.1 Conclusion

The current trend in wireless design is to simplify the analog front-end processing as much as possible and implement most of the fundamental functions using digital signal processing. This is mainly motivated by the ever increasing flexibility and integrability requirement as to multiple access wireless standards and services using a single, small size, low cost user equipments. As a consequence the traditional superheterodyne architecture is not the most appropriate choice and new receiver structures such as direct conversion receiver are under active investigation.

One of the most fundamental tasks of any radio receiver is to downcovert the desired channel signal from RF range to base band. In this context, the inherent image signal problem needs to be addressed with care. One interesting approach relaxing the requirements for RF filtering is to use IQ downcoversion. In practice, IQ imbalances are unavoidable in the analog front end, which results in finite and usually insufficient rejection of the image frequency band. This causes the image signal to appear as interference on the top of the desired signals.

An OFDM modulated RF signal is down converted to baseband through a direct conversion receivers with considerable IQ imbalances. The proposed algorithm is then applied on the resulting downconverted signals. Demodulation performance with and without the proposed compensation is compared to show the effectiveness of the proposed scheme. It was illustrated that the BER values for an OFDM system with typical (practical) IQ imbalances may be unacceptable. An important effect of IQ imbalances is that the achievable BER saturates as the SNR increases, suggesting that the systems performance at high SNR will be limited by the IQ imbalances rather than the SNR. The performance degradation becomes more severe at high SNR values and high density constellations.

The approach proposed in this thesis relies on using digital signal processing techniques to compensate for analog domain impairments (IQ imbalances) in the digital domain. As the main contribution, digital IQ imbalance compensation based on Least Square (LS) and Adaptive Least Mean (LMS) square are discussed in detail. There are several advantages associated with the

proposed digital schemes, with the main advantage being that they allow us to exploit the digital processing power to alleviate problems arising from analog imperfections.

The design of direct conversion receivers typically yields an IQ imbalance on the order of amplitude 1-2 % and phase imbalance of 1-2 degree[8][20]. The performance curves shown in figure 5.2-5.7 clearly demonstrate that for such IQ imbalance values, compensation is absolutely necessary to enable a high data rate communication. As shown in chapter five, the performance of the least square (LS) techniques is close to the ideal case. It is also shown that the performance of LMS techniques is based on the available number of training symbols. The need for longer training symbols is the drawback of LMS algorithm.

6.2 Future work

- One basic assumption in the derivation of the proposed algorithm is that the imbalance effects can be modeled as a linear system. In addition, it is assumed that there is no carrier frequency offset. In practical implementations, however, the non linear effects of the analog circuitry and carrier frequency offset can not be avoided. This may turn out to reduce the performance of the proposed approaches. This may constitute one important topic for future work and research.

- MIMO systems can provide higher effective SNR and consequently higher data throughput by enabling higher constellations sizes. However, at higher SNR values, the BER performance of the system is most probably limited by IQ imbalances. Thus studying the effects of IQ imbalance in MIMO OFDM system and developing appropriate compensation schemes could also be anther important topic for future work.

REFERENCE

1. J. Crols and M. S. J. Steyaert, “Low-IF topologies for high-performance analog front ends of fully integrated receivers,” IEEE Trans. on Circuits and Systems-II, vol. 45, pp. 269-282, March 1998.
2. B. Razavi, “Architectures and circuits for RF CMOS receivers,” Proc. IEEE Custom Integrated Circuits Conference, pp. 393-400, Santa Clara, CA, USA, May 1998.
3. Chi-wa Lo, Howard C.Luong , “2-V 900-Mhz Quadrature Coupled LC Oscillators With Improved Amplitude And Phase Matchings”, Proceedings of the 1999 IEEE International Symposium on Circuits and Systems, vol.2, pp.585-8, June 1999.
4. B. Razavi, “RF Microelectronics”. Englewood Cliffs, NJ: Prentice-Hall, 1998.
5. Kalle Kivekas, Aarno Passinen, Jussi Ryynanen, Jarkko Jussila and Kari Halonen, “calibration techniques for active BiCMOS Mixers”, IEEE journal of solid-state circuits,vol.37,pp.766-769,June 2002.
6. Z. Pengfei, N. Thai, C. Lam, D. Gambetta, C. Soorapanth, C. Baohong, S. Hart, I. Sever, T. Bourdi, A. Tham, and B. Razavi, “A direct conversion CMOS transceiver for IEEE 802.11a WLANs,” *ISSCC Dig. Tech. Papers*, pp. 354-355, Feb. 2003
7. L. Der and B. Razavi, “A 2-GHz CMOS image-reject receiver with LMS calibration”, IEEE journal of Solid-State Circuits, vol. 38, no. 2, pp. 167–175, Feb. 2003.
8. M. Valkama, M. Renfors and V. Koivumen, “Advanced Methods for IQ imbalance Compensation in communication receivers”, IEEE transaction on signal processing, Vol.49, No 10, October 2001.
9. Bahzad Razavi, “CMOS Technology characterization for analog and RF design”, IEEE journal of solid-state circuts, vol.34, No 3, March 1999.
10. H. Moose, “A Technique for Orthogonal Frequency Division Multiplexing Frequency Offset Correction,” IEEE Trans. Comm., vol. 42, pp. 2908–2914, Oct. 1994.
11. J. H. Yu and Y. T. Su, “Pilot-Assisted Maximum-Likelihood Frequency-Offset Estimation for OFDM Systems”, IEEE Trans. Comm., vol. 52, pp. 1997–2008, Nov. 2004.
12. A. A. Abidi, “Direct-conversion radio transceivers for digital communications”, IEEE journal of Solid-State Circuits, pp. 1399-1410, December 1995.
13. M J. M. Pelgrom, A. C. J. Duinmaijer, and A. P. G. Welbers, “Matching properties of MOS transistors”, IEEE journal of Solid-State Circuits, pp.1433-1439, October 1989.

14. “IEEE WLAN: 802:11a: STND, Part 11: Wireless LAN medium access control (MAC) and physical layer (PHY) specifications: High-speed physical layer in the 5-GHz band”, IEEE, Piscataway, NJ, 1999.
15. “IEEE 802.11g, Part 11: Wireless LAN medium access control (MAC) and physical layer (PHY) specifications: Further higher-speed physical layer extension in the 2.4 GHz band”,IEEE, Piscataway, NJ, 2003.
16. “IEEE 802.16, Wireless Metropolitan Area Networks (Wireless MAN)”, IEEE, Piscataway, NJ.
17. “ETSI EN 300, Digital Video Broadcasting (DVB): Framing structure, channel coding and modulation for digital terrestrial television”, EN 300, ETSI, 2001.
18. “IEEE 802.15, Wireless Personal Area Networks (WPAN) High Rate Alternative PHY. Task Group 3a (TG3a)”, IEEE, Piscataway, NJ.
19. “IEEE 802.20, Mobile Broadband Wireless Access (MBWA)”, IEEE, Piscataway, NJ.
20. Behzad Razavi, “Design considerations for direct conversion receivers”, IEEE transaction on circuits and systems II”, vol. 44, No 6, June 1997.
21. R. W. Chang, “Synthesis of band-limited orthogonal signals for multichannel data”,BSTJ, pp.1775-1797, Dec. 1966.
22. B. R. Saltzburg, “Performance of efficient parallel data transmission systems”, IEEE Trans. on Comm. Tech., pp. 805-811, Dec. 1967.
23. S. B. Weinstein and P. M. Ebet, “Data transmission by frequency-division multiplexing using discrete Fourier transform”, IEEE Trans. on Communications, pp. 628-634, Oct.1971.
24. Tim C.W. Schenk, peter F.M. Smulders and Erik R.Fledderous, “Multiple carriers wireless Communication –Curse or Blessing”, Tijdschrift Ned. Elektron.& Radiogenoot (NERG), vol.70, No.4, pp. 112-123, Dec. 2005.
25. Jack P. F. Glas. “Digital I/Q imbalance compensation in a Low-IF receiver.” in proc. IEEE Global Communications Conference, volume 3, pages 1461–1466, Nov. 1998.
26. A.Baier, “Quadrature mixer imbalances in digital TDMA mobile radio receivers.” in Proc. international Zurich Seminar on Digital Communications, Electronic Circuits and Systems for Communications, pp 147-162., Mar 1990.
27. C. L. Liu., “Impact of I/Q imbalance on QPSK-OFDM-QAM detection.” IEEE Trans. Consumer Electronics, vol. 44, pp. 984-989, Aug 1998.

28. J. Maligeorgos, J. Long, “A 2 V 5.1-5.8 GHz image-reject receiver with wide dynamic range.”, 2000 IEEE International Solid-State Circuits Conference, Digest of Technical Papers, San Francisco, CA, USA, 7-9 Feb. 2000.
29. J. Long, J. Maligeorgos, “A 1 V 900 MHz image-reject downconverter in 0.5 μm CMOS”, CICC 1999, p.665-668, May 1999.
30. R. Montemayor, B. Razavi, “A Self-Calibrating 900-MHz CMOS Image-Reject Receiver”, ESSCIRC 2000, pp. 292-295, Sept. 2000.
31. J. Rudell, “A 1.9GHz Wide-Band IF Double Conversion CMOS Receiver for Cordless Telephone Applications”, IEEE Journal of Solid-State Circuits, p.2071-88., December, 1997.
32. T. May and H. Rohling, “Reducing the peak-to-average power ratio in OFDM radio transmission systems”, in Proc. IEEE Veh. Techno. Conf., vol. 3, pp. 2474-2478, Ottawa, Ont., Canada, May 1998.
33. Muller and J. Huber, “A comparison of peak power reduction schemes for OFDM”, in Proc. IEEE Global Telecommunications Conf., vol. 1, pp. 1-5, Phoenix, AZ, USA, Nov. 1997.
34. P. H. Moose, “A technique for orthogonal frequency division multiplexing frequency offset correction”, IEEE Trans. on Communications, vol. 42, No.10, pp.2908-2914, Oct. 1994.
35. Peled and A. Ruiz, “Frequency domain data transmission using reduced computational complexity algorithms,” *Proc. IEEE ICASSP*, pp. 964-967, Denver, CO, 1980.
36. Srihari Adireddy, Lang Tong , Harish Viswanathan ,“optimal placement of training for frequency-selective block-fading channels”, IEEE transactions on information theory, vol. 48, No. 8, august 2002.
37. Robert. G. Gallagher, “Information Theory and Reliable Communication”, Wiley, New York, 1968.
38. Ahmad R.S.Bahai and Burton R.Saltzberg, “multi-carrier digital communications, theory and application of OFDM”, New Jersey, Algorex Inc., 2002.
39. J. G. Proakis, Digital Communications, 3rd ed., McGraw-Hill, New York, 1995.
40. Pan Liu,Yeheskel Bar-Ness and Jianming Zhu,“Effects of Phase Noise at Both Transmitter and Receiver on the Performance of OFDM Systems ”,IEEE 2006 40th annual conference on information sciences and systems, pp. 312-316, Princeton, USA, March 2006.
41. Julius O. Smith III, “Mathematics of the Discrete Fourier Transform (DFT)”, Book Surge Publishing, California, March 15, 2002.

42. Marcus Windisch and Gerhard Fettweis, “Preamble Design for an Efficient I/Q Imbalance Compensation in OFDM Direct Conversion Receivers”, in Proceedings of the 10th International OFDM-Workshop (InOWo'05), Hamburg, Germany, September 2005.
43. Marcus Windisch, Gerhard Fettweis, “Performance Degradation due to I/Q Imbalance in Multi-Carrier Direct Conversion Receivers: A Theoretical Analysis”, in Proceedings of the IEEE International Conference on Communications (ICC'06), Istanbul, Turkey, June 2006.
44. Jan-Jaap Van de Beek, Ove Edfors, Magnus Sandell, Sarah Kate Wilson,Per Ola Borjesson, “On Channel Estimation in OFDM System”, proc. of vehicular Technology conference (VTC ’95),vol.2,pp.815-819,Chicago,USA,Septemebr 1996.
45. Monson H. Hayes, “Statistical Digital Signal Processing and Modeling”, John Wiley Sons, Inc., 1996.
46. S.J. Orfandis, “Optimum Signal Processing”, 2nd ed., McGraw-Hill, New York, 1988.
47. T. Pollet ,M van Bladel and Moeneclaey, “BER Sensitivity of OFDM Systems to carrier Frequency offset and Wiener Phase Noise”, IEEE Trans. on comm.,vol.43 No 2/3/4,pp.191-193, feb.1995.
48. M. Pauli and H.P.Kuchenbecker, “Minimization of the intermodulation distortion of a Nonlinearly Amplified OFDM Signal”, in proc. IEEE International communications Conf. (ICC), pp.1304-1307, June 1998.
49. C .Rapp, “Effects of HPA-Nonlinearity on a 4 DPSK/OFDM signal for a digital sound broadcasting system”, in proc. of the second European conference on satellite communication, Liege, Belgium, pp.179-184, oct.22-24, 1991.
50. H. Takanashi and R.van Nee, “Merged OFDM physical layer specification for the 5 GHZ band”, IEEE p802.11-98/72-rl, pp. 1-27, March 1998.
51. Ramjee Parasad, “OFDM for wireless multimedia communications”, Artech House Inc., Norwood, 2004.